[redacted]

CENTRAL RESEARCH LIBRARY
DOCUMENT COLLECTION

AEC RESEARCH AND DEVELOPMENT REPORT

ANP LIMITED DISTRIBUTION
ORNL-1944
Progress

MARTIN MARIETTA ENERGY SYSTEMS LIBRARIES
3 4456 0361000 0

92A

C-84

DECLASSIFIED

CLASSIFICATION CHANGED TO:
BY AUTHORITY OF: AEC 10-22-59
BY: E. Lackenmeister 1-19-60

SOLID STATE DIVISION

SEMIANNUAL PROGRESS REPORT

FOR PERIOD ENDING AUGUST 31, 1955

CENTRAL RESEARCH LIBRARY
DOCUMENT COLLECTION

LIBRARY LOAN COPY

DO NOT TRANSFER TO ANOTHER PERSON

If you wish someone else to see this document, send in name with document and the library will arrange a loan.

OAK RIDGE NATIONAL LABORATORY
OPERATED BY
UNION CARBIDE NUCLEAR COMPANY
A Division of Union Carbide and Carbon Corporation
UCC
POST OFFICE BOX P · OAK RIDGE, TENNESSEE

RESTRICTED DATA
This document contains Restricted Data as defined in the Atomic Energy Act of 1946. Its transmittal or the disclosure of its contents in any manner to an unauthorized person is prohibited.

[redacted]

[redacted]

ORNL-1944

ANP Limited Distribution

This document consists of 36 pages.
Copy 92 of 163 copies. Series A.

Contract No. W-7405-eng-26

SOLID STATE DIVISION

SEMIANNUAL PROGRESS REPORT

For Period Ending August 31, 1955

D. S. Billington, Director

J. H. Crawford, Jr., Assistant Director

DATE ISSUED

NOV 3 1955

OAK RIDGE NATIONAL LABORATORY
Operated by
UNION CARBIDE NUCLEAR COMPANY
A Division of Union Carbide and Carbon Corporation
Post Office Box P
Oak Ridge, Tennessee

[redacted]

MARTIN MARIETTA ENERGY SYSTEMS LIBRARIES

3 4456 0361000 0

[redacted]

ANP Limited Distribution
ORNL-1944
Progress

INTERNAL DISTRIBUTION

1. C. D. Baumann
2. R. G. Berggren
3. J. C. Betterton, Jr.
4. D. S. Billington
5. D. [illegible]der
6. T. [illegible] Blewitt
7. C. [illegible] Bopp
8. B. [illegible]orie
9. G. [illegible] Boyd
10. E. [illegible]oyle
11. H. [illegible]oks (consultant)
12. W. [illegible] Browning
13. W. E. Brundage
14. D. W. Cardwell
15. C. E. Center
16. R. A. Charpie
17. J. W. [illegible]leland
18. G. H. [illegible]lewett
19. A. F. Cowen
20. D. D. Cowan
21. J. H. [illegible]rawford, Jr.
22. F. L. [illegible]uller
23. J. E. [illegible]unningham
24. R. R. [illegible]ickison
25. S. E. [illegible]ismuke
26. L. B. [illegible]mlet (K-25)
27. M. J. [illegible]eldman
28. J. H. Frye, Jr.
29. J. [illegible] Gabbard
30. R. [illegible] Gray
31. W. [illegible] Harms (consultant)
32. C. [illegible] Harrill
33. A. [illegible]llaender
34. D. [illegible] Holmes
35. A. [illegible] Householder
36. J. [illegible] Howe
37. L. [illegible] Jetter
38. R. [illegible] Johnson
39. R. [illegible] Jones
40. W. [illegible] Jordan
41. G. [illegible]eilholtz
42. C. [illegible]eim
43. M. [illegible]elley
44. R. H. [illegible]ernohan
45. E. M. [illegible]ng
46. H. V. [illegible]ius
47. G. E. Klein
48. T. A. Lincoln
49. S. C. [illegible]ind
50. R. S. Livingston
51. H. G. MacPherson (consultant)
52. W. D. Manly
53. A. [illegible] Miller
54. E. [illegible]. Miller
55. J. [illegible]. Morgan
56. K. [illegible]. Morgan
57. E. [illegible]. Murphy
58. J. [illegible]. Murray (Y-12)
59. R. [illegible]. Oliver
60. W. [illegible]. Parkinson
61. P. [illegible] Reyling
62. M. [illegible] Robinson
63. H. [illegible] Schweinler
64. F. [illegible]itz (consultant)
65. E. [illegible] Shipley
66. O. [illegible]sman
67. M. [illegible] Skinner
68. G. [illegible] Smith
69. A. [illegible] Snell
70. R. [illegible] Sproull (consultant)
71. E. [illegible] Stansbury
72. D. [illegible] Stevens
73. W. [illegible]turm
74. C. [illegible]usano
75. J. A. [illegible]wartout
76. E. [illegible]aylor
77. J. B. [illegible]rice
78. F. [illegible]onderLage
79. J. [illegible]arde
80. C. [illegible] Webster
81. M. S. Wechsler
82. R. [illegible] Weeks
83. A. [illegible]. Weinberg
84. E. P. Wigner (consultant)
85. G. C. Williams
86. W. R. Willis
87. J. [illegible]. Wilson
88. C. E. Winters
89. M. [illegible]. Wittels
90. B[illegible]gy Library
91-93. C[illegible]al Research Library
[illegible] H[illegible]h Physics Library
[illegible] [illegible]rds Department
[illegible] L[illegible]ratory Records, ORNL R.C.

[redacted]

[redacted]

101. ORNL Document Reference Library, Y-12 Branch
102. Reactor Experimental Engineering Library

EXTERNAL DISTRIBUTION

103. AFDRD
104. AFDRQ
105. AFSWC
106. Aircraft Lab WADC (WCLS)
107. Argonne National Laboratory
108. Assistant Secretary – Air Force, R & D
109. ATIC
110-112. Atomic Energy Commission, Washington
113. BAGR – WADC
114. Boeing – Seattle
115. BuAer – Keller
116. Chief of Naval Research
117-119. Col. Gaster (WCSN)
120. Convair – San Diego
121-123. CVAC – Fort Worth
124. Director of Laboratories (WCL)
125. Director of Weapons Systems, ARDC
126. Douglas
127. East Hanford Area Office
128. Equipment Laboratory – WADC (WCLE)
129-132. GE-ANP
133. Glenn L. Martin
134. KAPL
135. Lockheed – Burbank
136. Lockland Area Office
137. Los Alamos Scientific Laboratory
138. Maintenance Engineering Services Division – AMC (MCMTA)
139.140. Materials Lab (WCRTO)
141. NACA – Cleveland
142. NACA – Washington
143. NDA
144. North American – Aerophysics
145. Patent Branch, Washington
146-148. Power Plant Laboratory – WADC (WCLPU)
149-152. Pratt & Whitney
153. Rand
154. RDG – Sutherland
155. SAM
156-157. Technical Information Service, Oak Ridge Operations Office
158-160. WADC Library
161. WAPD – Bettis Plant
162. Wright Aero
163. Division of Research and Medicine, AEC, ORO

[redacted]

[redacted]

Reports previously issued in this series are:

ORNL-1025	Period Ending January 31, 1951
ORNL-1095	Period Ending April 30, 1951
ORNL-1128	Period Ending July 31, 1951
ORNL-1214	Period Ending October 31, 1951
ORNL-1261	Period Ending January 31, 1952
ORNL-1301	Period Ending May 10, 1952
ORNL-1359	Period Ending August 10, 1952
ORNL-1429	Period Ending November 10, 1952
ORNL-1506	Period Ending February 10, 1953
ORNL-1606	Period Ending August 31, 1953
ORNL-1677	Period Ending February 28, 1954
ORNL-1762	Period Ending August 30, 1954
ORNL-1851	Period Ending February 28, 1955

[redacted]

[redacted]

CONTENTS

SUMMARY 1

RADIATION METALLURGY 3

ANP Creep and Stress Corrosion 3

ENGINEERING PROPERTIES 5

LITR Fluoride-Fuel Loop 5

FUSED SALTS 16

LITR Vertical Dynamic-Corrosion Loop 16

Deposition of Ru^{103} and Nb^{95} from Fluoride Fuels 17

Theoretical Treatment of Xe^{135} Poisoning in the ARE and the ART 18

Delay of Noble Gases by Charcoal Traps 18

SPECIAL PROJECTS 23

Hot-Cell Operation 23

Hot Metallography 24

[redacted]

[redacted]

SOLID STATE DIVISION SEMIANNUAL PROGRESS REPORT

SUMMARY

RADIATION METALLURGY

ANP Creep and Stress Corrosion. – Irradiation of a creep apparatus with Inconel specimens at 1500 psi was completed at the MTR. Because of partial failure of the extensometer, the total creep will be measured when the apparatus is returned to Oak Ridge.

ENGINEERING PROPERTIES

LITR Fluoride-Fuel Loop. – The Inconel loop was dismantled for removal of the samples and for recovery of the uranium by using the remote cutting tools installed in a hot cell of the Solid State Building. Disassembly proceeded without incident. An electric-arc cutting technique was developed for removal of the stainless steel enclosure around the pump bowl. Fission power and maximum flux were determined by irradiating a simulated loop, by heat-balance calculations, by radiochemical analyses for fission products in the fuel, by measuring the activation of cobalt foils attached to the loop, and by activation of the loop tubing itself. The determinations of the power by these various methods gave 2.5 to 2.8 kw during operation of the loop, and the maximum power density was 0.4 kw/cc.

Chemical analyses of the fuel were carried out to determine U, Zr, and the major constituents of Inconel: Ni, Cr, and Fe. There were no appreciable changes in the composition of the fuel during operation, other than dilution of the fuel with the $NaF\text{-}ZrF_4$ mixture used to flush the system prior to irradiation. The chromium content had increased; whereas nickel probably had decreased slightly during operation, in keeping with experience with unirradiated loops. An examination for ruthenium fission product showed that this element had plated out of the fuel onto the tubing walls.

Corrosion of the Inconel by the fluoride salt was relatively light, as revealed by metallographic examination of the loop tubing. The corrosion was fairly general and uniform, and there was no acceleration of attack that could be attributed to the effects of irradiation. The average depth of voids was generally ½ mil, but it was 1 mil in one region which was not in the irradiated section. At surface cracks there was corrosive penetration to a depth of 4 mils, but cracks with almost this same depth of penetration were found in the as-received tubing. No mass-transferred material was observed, reflecting the almost isothermal conditions of operation.

FUSED SALTS

LITR Vertical Dynamic-Corrosion Loop. – The vertical dynamic-corrosion loop operated 30 hr in the LITR and was terminated because of a brush failure in the motor. The operating characteristics of the loop followed the design calculations satisfactorily. The next loop, which will have an induction-type motor and some minor design changes, will allow more fuel to be in the active lattice.

Deposition of Ru^{103} and Nb^{95} from Fluoride Fuels. – Gamma-ray scintillation-spectrometry analyses show that Ru^{103} and Nb^{95} deposited from fluoride fuels. The results are consistent with those from the horizontal fluoride loop operated in the LITR and with those from the operation of the ARE. An autoradiograph indicates that the Ru-Nb mixture does not diffuse readily into Inconel under ARE conditions.

Theoretical Treatment of Xe^{135} Poisoning in the ARE and the ART. – A theoretical study has been made of the kinetics of Xe^{135} poisoning in ANP-type reactors. The calculated dependence of the steady-state Xe^{135} poisoning on the sparging-gas flow rate is illustrated. The time dependence of Xe^{135} poisoning during reactor operation has been studied extensively.

Delay of Noble Gases by Charcoal Traps. – Charcoal traps can be used as a time delay for noble gases in a flowing system. Experiments were performed to provide actual data for the design of such a trap, and it is now being used in a fission-product off-gas line operating at room temperature. In these experiments a small pulse of Kr^{85} was swept through the trap with air, and, upon observing, downstream from the trap, the activity as a function of time, it was found that the krypton was delayed. The peak activity of the eluted gas occurred after a time delay which was

[redacted]

directly proportional to the trap volume and inversely proportional to the air flow rate.

SPECIAL PROJECTS

Hot-Cell Operation. – Experiments were performed involving the disassembly of HRP in-pile loops FF, GG, EE, and the LITR fluoride-fuel loop. Equipment was installed for the disassembling of the vertical dynamic-corrosion loop. Another significant experiment consisted in removing fuel plates from an LITR fuel element. Pratt and Whitney Aircraft solid-fuel-element capsules (PW-1-12 and PW-1-13) were opened, and the samples were removed; however, postirradiation studies have not yet been completed. Impact and tensile measurements were conducted on various metals for both the ANP and the HRP.

Hot Metallography. – Metallographic examination of HRP in-pile loop FF has been completed. Corrosive attack was light and was consistent with that which occurred in previous loops.

Corrosive attack, as shown by examination of sections from the LITR fluoride-fuel loop No. 2, was light, with maximum penetration of approximately 1½ mils at a location 3½ ft from the nose of the loop.

Examination of GE-ANP fuel elements 3O and 3U revealed that failure during irradiation was not due to radiation damage but was a result of faulty fabrication techniques.

Metallographic examination of an MTR fuel element which had failed in operation indicated that failure was caused by environment rather than by radiation damage.

Experiments with sections of an LITR fuel element resulted in the conclusion that bending of fuel elements for ease in chemical processing was not feasible, since the bends required were beyond the ductility limits of the plates.

The construction and the installation of equipment for the extension of the remote metallographic facility have been completed, and operation has begun. The extension of the original metallographic cell permitted the metallographic process to be divided into essentially three separate operations, which resulted in greater ease in remote manipulation. Modular construction was utilized in the major portion of the standard metallographic equipment. This will allow equipment repairs to be made with a minimum of personnel irradiation. Installation of a B&L research metallograph will allow metallographic examination to be made with polarized light and dark-field illumination, in addition to bright-field illumination. A B&L stereorelay will allow three-dimensional viewing and photography in the range ½X to 30X.

RADIATION METALLURGY

J. C. Wilson

ANP CREEP AND STRESS CORROSION

W. W. Davis J. C. Zukas
N. E. Hinkle J. C. Wilson

The reactor Experimental Review Committee approved the insertion of the pressurized stress-corrosion apparatus in facility HB-3 of the LITR. The apparatus, briefly described previously,[1] is shown in Fig. 1. A thin-walled tubular specimen, surrounded by an annulus containing approximately 2.5 g of enriched fuel, is internally stressed by helium gas admitted through the pressure chamber while being maintained at a temperature of 1500°F. The heat generated by the fissioning fuel is conducted out through fins to a water-cooling coil. A resistance heater spaced between the fins is intended to provide some measure of control of the specimen temperature as long as the reactor is up to power. The control thermocouple on the inside of the specimen tube should read very nearly the maximum temperature of the system at any time. Heat-transfer calculations predict that the fuel will be frozen at the outer walls of the fuel chamber, so that the molten fuel will then be contained in a cup of solid fuel, thus lowering the surface-to-volume ratio of the test system considerably. It does not appear likely at this time that the temperature of the specimen can be maintained at control level during reactor shutdown periods; fuels with a power density of 1000 w/cc are difficult to simulate in bench tests of this type of experiment. The gas space above the fuel is connected through a capillary to an expansion chamber in order to decrease the back pressure on the specimen walls when the specimen is brought up to temperature. The first group of specimen assemblies is now being filled with fuel for tests in the LITR. Engineering of the plug designed to adapt the test to the MTR is under way.

A simplified version of the apparatus which will permit creep data to be obtained in any combination of two nonfuel atmospheres is undergoing bench tests prior to irradiation. The same specimen tube is used for both tests.

Measurements of the total strain in the specimen tubes will be accomplished with a pneumatic measuring gage. The gage has been received and tested. Inside-diameter measurements of the specimen tube can be made with an accuracy of about 0.00005 in. with the pneumatic gage, and the manipulative operations are simple enough to be done in a hot cell.

The operation of a number of pressure-reducing valves, with pressure ranges from 200 to 1000 psi, has been checked over a period of about a week. Of the two valves presently undergoing test, one appears capable of holding set pressures within 1% over the range of room temperatures encountered in the laboratory.

A 1:1 ratio pressure-volume transformer for isolating the gas inside the specimen tube from the pressure supply has been built and tested.

Fig. 1. Exploded and Assembled Views of Pressurized Stress-Corrosion Apparatus.

[1] W. W. Davis *et al.*, *Solid State Semiann. Prog. Rep. Feb. 28, 1955*, ORNL-1851, p 3.

Because of the controlled, limited volume of gas available to the specimen tube with this apparatus, leakage or rupture results in only a very small pressure rise in the whole apparatus. Protection against pressure rises in the water-cooled irradiation experiment will, in this manner, greatly reduce the weight of the irradiation can.

A low-cost, versatile transfer shield was designed and built for transporting fuel-containing apparatus from the LITR to the Solid State Building.

The MTR tensile creep-test apparatus was irradiated at 1500°F and 1500 psi for two cycles in hole HB-3 of the MTR. For some unknown reasons, two of the four Bourdon-tube extensometers did not operate after insertion into the reactor. Therefore, total creep measurements and the determination of the effects of radiation on the calibration factors of the Bourdon-tube extensometers will be made when the apparatus is returned to ORNL. The experimental assembly has been cut from the irradiation plug at the MTR site. The bench test, equivalent to the in-pile rig in respect to time, temperature, and stress, is assembled, and testing has started.

ENGINEERING PROPERTIES

O. Sisman

LITR FLUORIDE-FUEL LOOP

W. E. Brundage
C. D. Baumann
R. M. Carroll
J. R. Duckworth
C. Ellis
J. G. Morgan
M. T. Morgan
A. S. Olson
W. W. Parkinson

High power densities and effective heat transfer are paramount requirements in the development of light, high-temperature power reactors. To provide a system meeting these requirements, circulating molten-salt fuels have been investigated extensively, and corrosion problems have proved to be of primary importance. The effect of neutron irradiation on the corrosion and fuel stability in a dynamic molten-salt system has been studied by circulating a fluoride-fuel mixture through a loop of Inconel tubing in hole HB-2 of the LITR. The fabrication of the parts for this loop, its instrumentation, and its assembly have been described earlier,[1] and the record of operation of the loop has been presented in the previous progress report.[2] A recapitulation of the operating conditions follows: the temperatures were 1450 to 1500°F; Reynolds number was 4500 to 5200 (about 5000 for most of the operation); power generation was about 2.8 kw; the duration of operation was 645 hr, with the reactor at full power (3 Mw) for 475 hr.

Before the loop could be pulled from the reactor into the withdrawal shield, it was necessary to separate the pump from the loop because of its size. A hydraulic shear incorporated in the operating shield was used for cutting the fuel tubes and electrical leads between the reactor shield and the pump. The pump was then rolled away in its operating shield, which also served for storage.

The loop was removed from the LITR into a horizontal, cylindrical shield and was transferred to a hot cell at the Solid State Building. To accomplish this, a door was installed in the rear wall of the hot cell (Fig. 2). A system of wire cables installed in both the shield and the hot cell provided for the withdrawal of the loop from the shield into the hot cell and for the return of the loop or, if necessary, its disassembled parts into the shield. The equipment for dismantling the irradiated loop, as arranged in the hot cell, was shown in the previous report.[3] The primary cutting instrument was a horizontal band saw of 8- by 10-in. capacity adapted for remote operation. The saw was fitted with a hydraulic vise and with an off-gas system which, to prevent the spread of radioactive fuel, collected the saw cuttings both from a hopper beneath the cut and directly from the blade. In this latter collecting operation, some air cooling was substituted for the normal water cooling of the saw blade. A portable electric hacksaw, having its own hydraulic vise and operable on the manipulator, was used only for cuts inaccessible to the band saw. A more frequently used tool was a pair of "hawk-bill" sheet-metal hand shears which were adapted for hydraulic operation and which were attached to a special set of manipulator tongs. An electric impact wrench, also operable on the manipulator, completed the group of disassembly tools, except for a cutting electrode which was used on the pump. The impact wrench could be fitted with various sizes of sockets and extension rods and was used to remove the cap screws holding the closure flange on the rear of the loop jacket. This operation (after pulling the loop from the shield into the hot cell) is shown in Fig. 3.

Disassembly of the loop was carried out by first stripping away all thermal insulation, lead wires, heaters, shielding, and structural materials, and then cutting the fuel tubes into lengths just short enough to permit the loop to be drawn from its jacket into the hot cell. The mouth of the jacket was held in the band-saw vise, and the loop was withdrawn in stages under the saw blade. In this way the loop tubing and support rods were conveniently cut, and the prior stripping avoided the mixing of radioactive fuel with debris from the loop. The loop as it appeared during this stripping operation is shown with the hydraulic shears in Fig. 4. After extraneous material was removed from the fuel tubes, 22 tube sections were cut from appropriate locations around the loop for metallographic examination. Additional tube sections were cut to provide samples of the fuel for

[1] W. E. Brundage *et al.*, *Solid State Semiann. Prog. Rep. Aug. 30, 1954*, ORNL-1762, p 21.

[2] W. E. Brundage *et al.*, *Solid State Semiann. Prog. Rep. Feb. 28, 1955*, ORNL-1851, p 7.

[3] *Ibid.*, p 12.

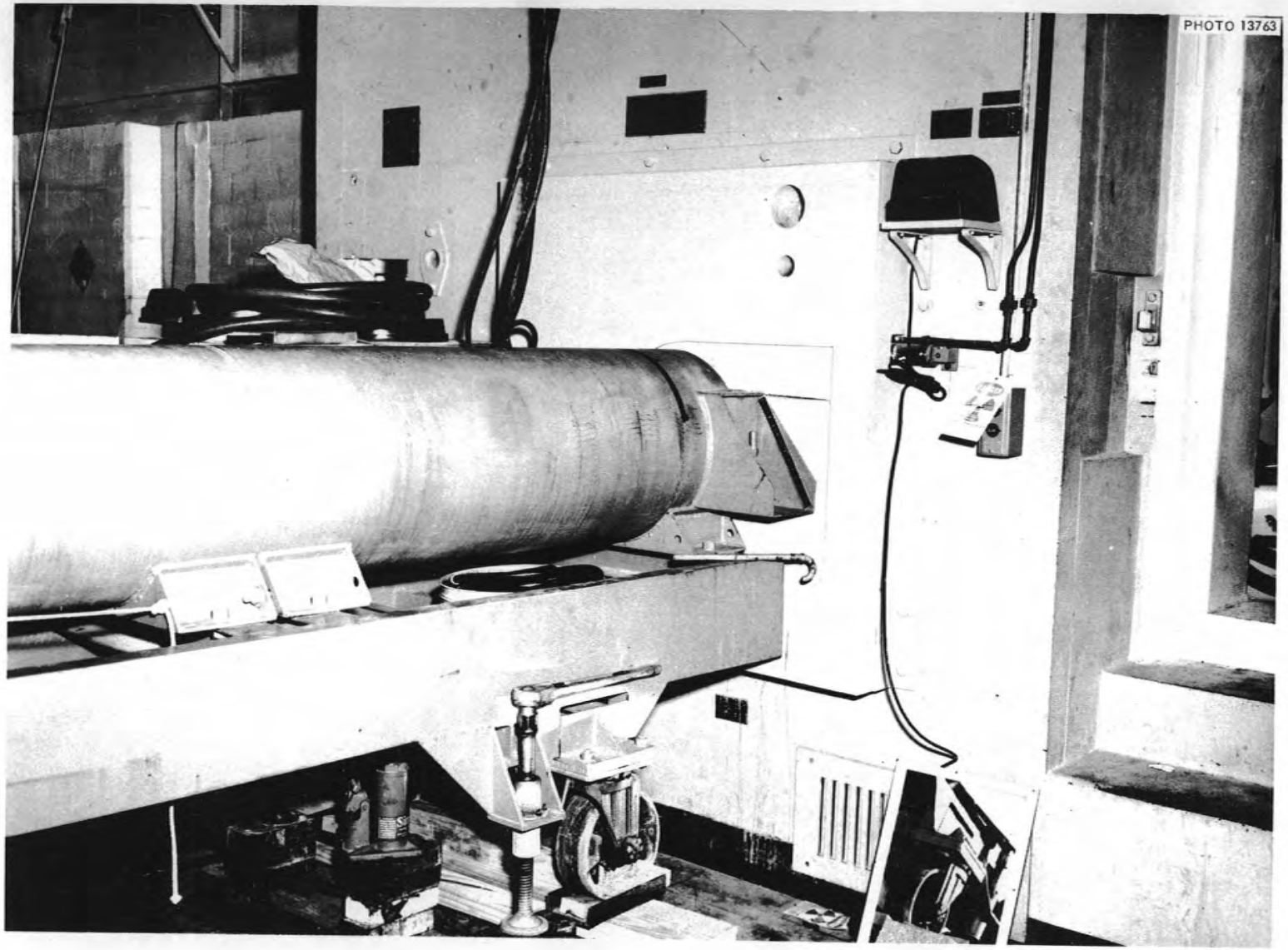

Fig. 2. Loop Withdrawal Shield in Position at Hot Cell.

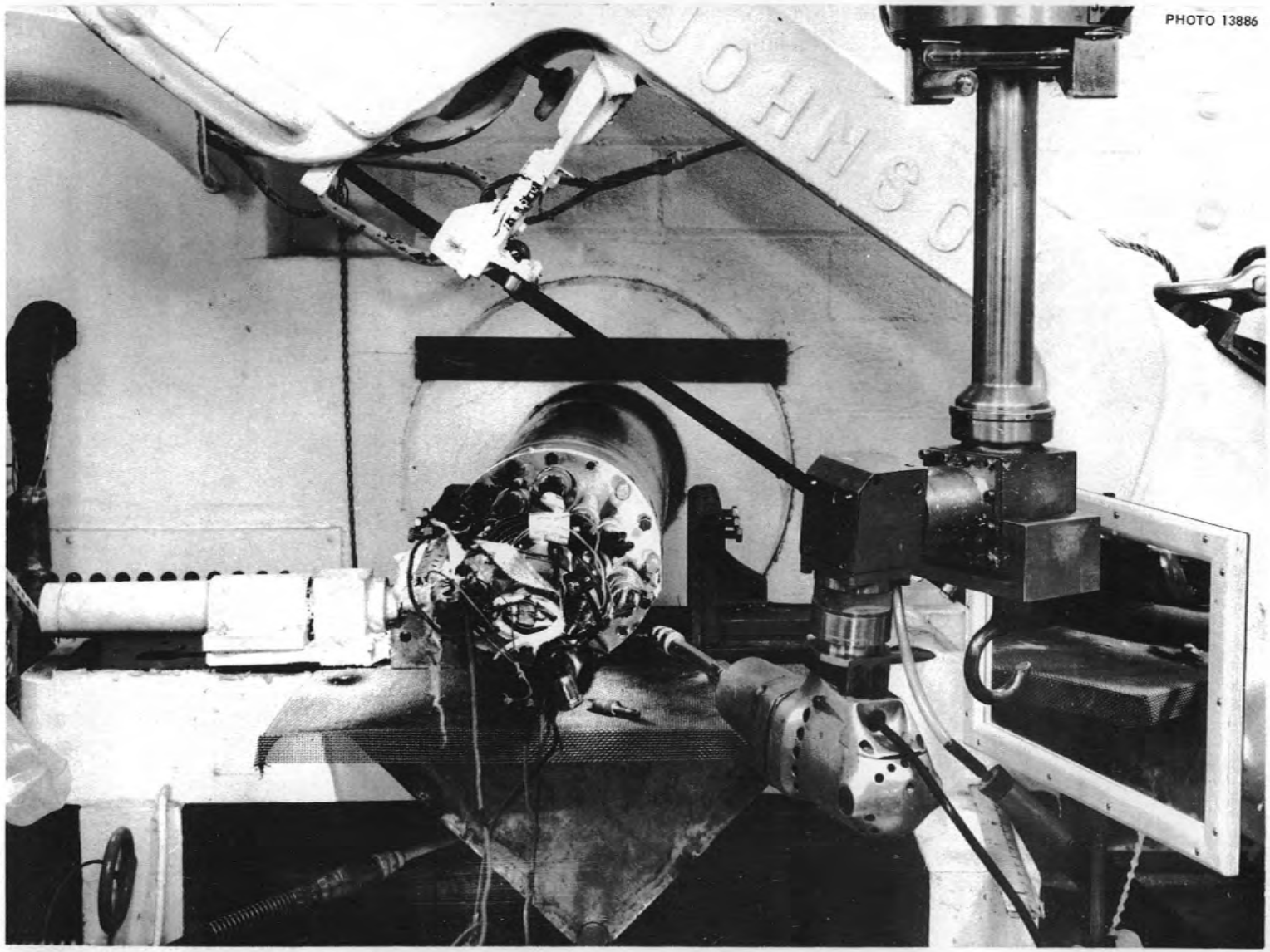

Fig. 3. Removal of Flange with Impact Wrench.

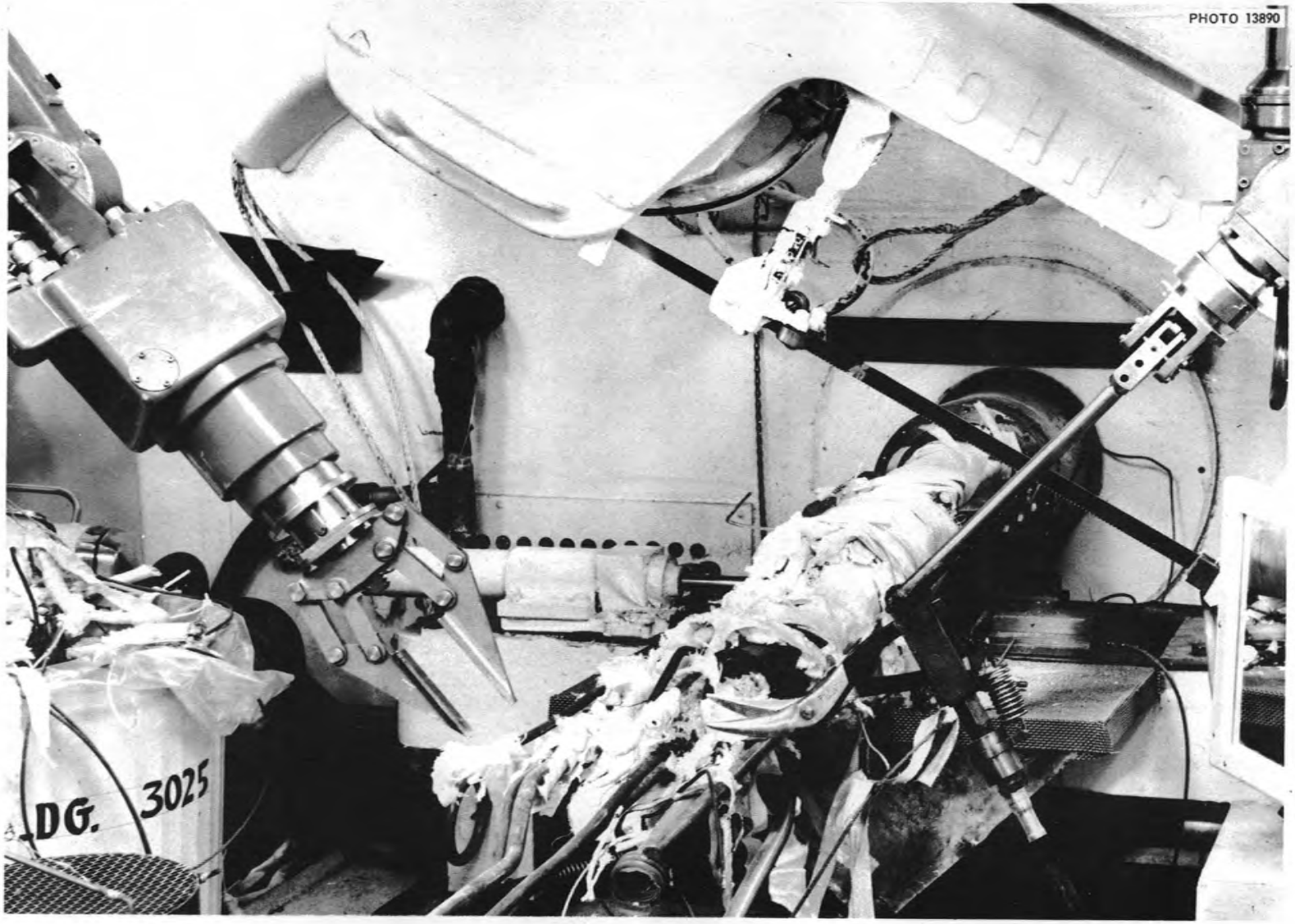

Fig. 4. Loop Partly Dismantled.

chemical analysis. The remaining tubing was packaged and taken to a storage area for future recovery of the uranium.

The pump, in its stainless steel, inert-atmosphere enclosure, was too large for handling in the band saw. In order to remove this enclosure, an electric welder was arranged so that cutting electrodes could be operated by the manipulators. After removal of the enclosure (Fig. 5) the pump was positioned in the band saw, and the inlet and discharge fuel lines were cut from the bowl. The bowl was then cut off at the solidified-fuel level and stored for uranium recovery. Radioactivity in the remaining portion of the pump made it advisable to save an additional portion of the bowl for fuel recovery also.

Measurement of the fission power generated in the loop during irradiation was discussed in the previous report.[2] Since the estimates from heat-balance measurements were unexpectedly low, an experiment was carried out to measure the flux depression in the fuel in a simulated loop nose-piece. An assembly duplicating the irradiated portion of the loop was made up and filled with a 2 wt % Cd-Pb alloy which had the same macroscopic absorption cross section as the fuel salt. This assembly was inserted into a water-cooled jacket in hole HB-2. The neutron activation of the cadmium alloy was measured, and the relation between the activation and the neutron flux was established by calibrating the alloy with cobalt foil. This flux determination gave considerably higher fission power in the loop than did the heat-balance measurements. One possible cause of the discrepancy was the uncertainty regarding the position of the loop in the hole, since the thermal expansion of the loop structure could not be predicted precisely. The flux distribution, however, did agree qualitatively with the measurements discussed below.

Another measurement of neutron flux was obtained from the activity of cobalt monitor foils which had been attached at various points along the loop. Since these foils were of necessity outside the fuel tube, measurements were also made of the activation of the Inconel fuel tube. The neutron flux was calculated from this activation by using the cross section measured by Bopp.[4] The neutron flux as determined by these two methods is plotted as a function of distance along the loop in Fig. 6. The fission power calculated

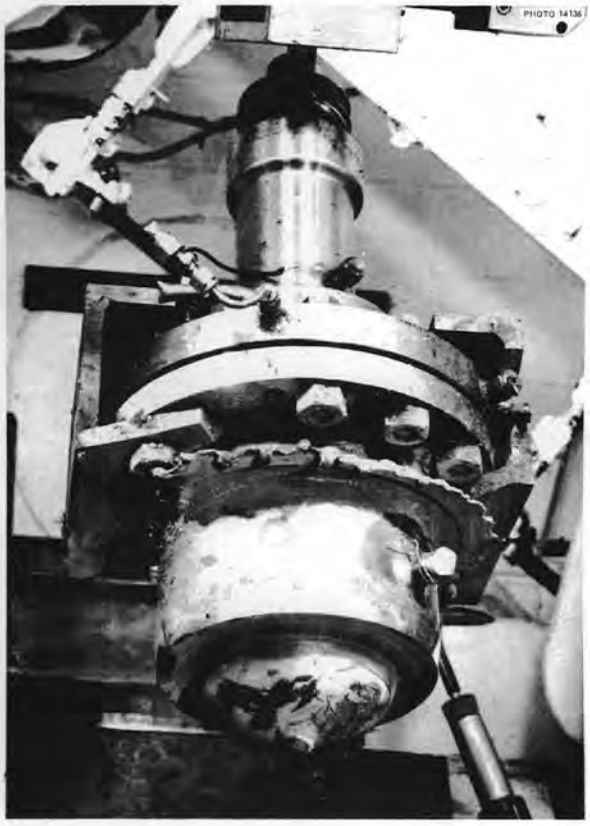

Fig. 5. Pump After Removal of Enclosure and Fuel Tubes.

[4]C. D. Bopp, *Gamma Radiation Induced in Engineering Materials*, ORNL-1371 (April 16, 1953).

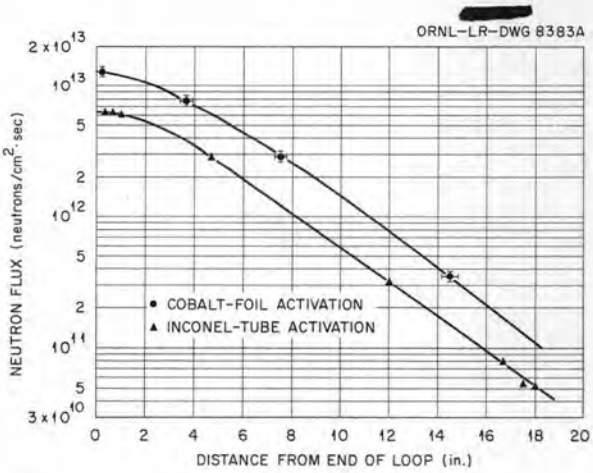

Fig. 6. Flux Incident on the LITR Fluoride-Fuel Loop.

from the Inconel activation was 2.8 kw, and the maximum power density was 0.4 kw/cc.

The fission power generated in the fuel was also determined by measuring the activities of fission products in the samples taken for chemical analysis. The activity of the fuel was measured in a gamma-ray spectrometer, and the height of the Zr-Nb peak was compared to that of a standard. The Zr-Nb concentration corresponded to a fission power of 2.0 kw. The zirconium fission product and the cesium product were also chemically separated from two of the samples, and the fission rate was estimated from their activities. The cesium samples resulted in estimates of 1.5 and 2.1 kw, which are considerably lower than the determinations by other methods. The power indicated by the cesium content is expected to be low, since it is known that the gaseous parent xenon escapes from the fuel mixture. The two separated zirconium samples indicated fission powers of 2.3 and 2.5 kw. In comparing the results of the zirconium determinations with the 2.8-kw value indicated by the electrical measurements and by the flux determinations, it should be kept in mind that the allowance for decay of the zirconium fission product during the reactor shutdowns was only approximate. From these determinations, then, the best estimates are that the total fission power generated in the loop was between 2.5 and 2.8 kw and that the maximum power density at the end of the loop was about 0.4 kw/cc.

The tube sections cut for chemical analysis of the fuel were taken from both the in-pile and out-of-pile parts of the loop to ensure representative samples. Analytical fuel samples were taken from the ends of the tube sections by drilling out solidified fuel with carbide-tipped bits. Clean samples were assured by collecting only the borings from a small bit after a large bit had been used to drill through surface material. Samples of fuel which had not been circulated during operation of the loop were obtained in the same manner from the portion of the loop filling line which was outside the pump shield. These samples were analyzed for U, Zr, and the constituents of Inconel: Ni, Cr, and Fe. The results are presented in Table 1. The nominal composition of the original fuel was 25 mole % (47 wt %) UF_4 enriched approximately 93%, 62.5 mole % NaF, and 12.5 mole % ZrF_4. It can be seen that the preliminary flushing and cleaning with NaF-ZrF_4 diluted the uranium in the operating charge of the loop. The analytical results show that the uranium concentration remained unchanged during the run, that the chromium content increased due to corrosion of Inconel, and that the nickel content probably decreased during the course of corrosion reactions. These changes in the concentration of Inconel components in the fuel and the corrosion attack discussed below are consistent with observations on unirradiated loops.[5]

Radioactivity measurements were made on two samples of the fuel for determination of the fission-product ruthenium content. The first was treated to separate the ruthenium, and its activity was measured. It showed less than 5×10^4 d/sec per gram of fuel, whereas the ruthenium activity as calculated from the fission power should have been of the order of 10^7. The second sample of the fuel was not separated, but its gamma emission was measured on a scintillation spectrometer.

[5]G. M. Adamson, R. S. Crouse, and P. G. Smith, *Examination of Inconel–Fluoride 30-D Pump Loop Number 4695-1*, ORNL CF-55-3-179 (March 28, 1955); G. M. Adamson and R. S. Crouse, *Examination of Fluoride Pump Loops 4930-A and 4935-1*, ORNL CF-55-4-181 (April 26, 1955).

TABLE 1. ANALYSIS OF FUEL SAMPLES FROM LITR FLUORIDE-FUEL LOOP*

Sample	U (%)	Zr (ppm)	Ni (ppm)	Cr (ppm)	Fe (ppm)
Original fuel	47.4		83	44	120
Fill line	43.9 ±1.9		240 ±120	10 ±10	85 ±15
Loop, in-pile	43.7 ±0.3	13.1 ±0.5	40 ± 10	140 ±20	120 ±20
Loop, out-of-pile	43.7 ±2.0	12.9 ±1.8	20 ± 10	150 ±30	180 ±80

*The deviation listed is the maximum variation from the mean of all samples except those obviously contaminated.

The ratio of the height of the ruthenium peak to that of the Zr-Nb peak was compared with a set of Ru-Zr standards. The fuel contained not over 0.03 as much ruthenium activity as Zr-Nb activity, whereas the calculated ratio was 0.16. Tube sections from the loop were given to M. T. Robinson and co-workers, who found five times as much ruthenium activity as Zr-Nb on the Inconel tube walls; yet the ruthenium should have been only 0.6 as much if the deposits on the walls were only traces of fuel.[6] Apparently, most of the fission-product ruthenium plated out on the container walls during operation, as was observed in the ARE.[7]

Tube sections cut from the loop for metallographic specimens were cleaned of fuel to facilitate polishing and etching. They were placed vertically in an inert-atmosphere furnace and maintained at above 750°C until drainage of the fuel was complete. The specimens received metallographic treatments by the method usually used for remote processing of Inconel samples. Metallographic preparation and examination were performed by the Remote Metallography Group of the Solid State Division under Feldman.[8] Control specimens (pieces of as-received tubing cut from the ends of the tubes used to fabricate the loop) were examined for comparison with the samples from the loop.

In general, the changes in the Inconel were those that would be expected in specimens subjected to the heat treatment imposed by the operation of the loop. Corrosion penetration averaged ½ mil. The penetration at those points from which specimens were taken is indicated in Fig. 7. No deposits of mass-transferred material were observed. Also shown in Fig. 7 are the locations at which the specimens pictured in Figs. 8 through 13 were cut. Figure 8 presents a typical sample from the short out-of-pile section of the loop – the only section unheated during irradiation. This sample was in the outlet leg of the loop and was maintained at about the temperature of the remainder of the loop, within the accuracy of the thermocouples, by the circulating fuel. Samples from this section of the loop showed the minimum corrosive attack; average penetration was less than ½ mil. A sample taken from the inlet leg in the reactor shield and typifying the entire unirradiated part of the loop is shown in Fig. 9. Penetration averaged ½ mil, and maximum penetration was 1 mil. Maximum corrosion in the loop was found in the unirradiated portion of the outlet leg (Fig. 10), where the average penetration was 1 mil and the maximum penetration 3 mils. The unused end of the tubing in this portion of the loop was the control specimen, which is shown in Fig. 11. Surface cracks

[6] M. T. Robinson, *Ru Deposition in In-Pile Loop*, ORNL CF-55-4-16 (April 5, 1955).

[7] M. T. Robinson, S. A. Reynolds, and H. W. Wright, *The Fate of Certain Fission Products in the ARE*, ORNL CF-55-2-36 (Feb. 7, 1955).

[8] M. J. Feldman *et al.*, *Metallographic Analysis of Fuel Loop II*, ORNL CF-55-6-22 (June 21, 1955).

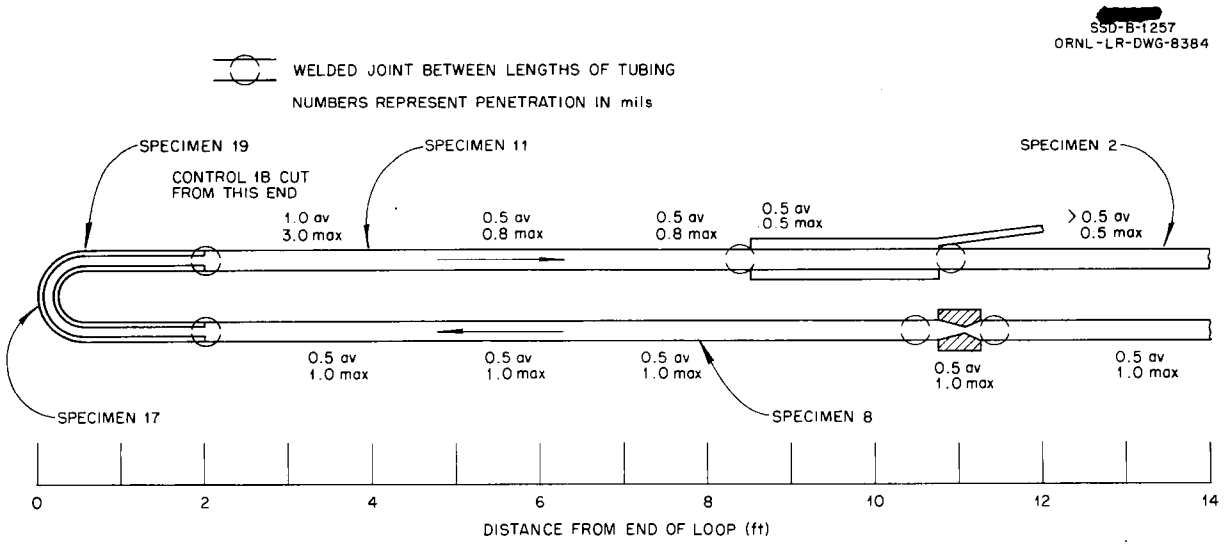

Fig. 7. Schematic Diagram of LITR Fluoride-Fuel Loop Showing Locations of Specimens and Welds.

on the inner surface of the tubing were observed to be common in the control pieces. These cracks were thought to be responsible for occasional voids extending to depths of 3 or 4 mils, since cracks of about the same depth and shape were found in the control specimens. A specimen from the irradiated section closest to the reactor lattice is shown in Fig. 12. The corrosion was about the average of that found elsewhere but without the occasional deep voids that resulted from surface cracks. The thick-walled tubing for the irradiated section was from a lot different from that used in the unirradiated sections. Another specimen from the irradiated section but from a lower flux region (Fig. 13) exhibited the same degree of corrosive attack but also exhibited a larger grain structure, possibly because of higher temperatures that resulted from better contact with the tubular heaters. No enhancement of corrosion by irradiation or other unusual effects were noted in the loop. These observations are in agreement with the findings from some of the capsule irradiations.[9]

The experimental work on this project has been completed, and a topical report is being prepared.[10]

[9] W. E. Browning, *Solid State Semiann. Prog. Rep. Aug. 30, 1954*, ORNL-1762, p 39.

[10] O. Sisman, W. E. Brundage, and W. W. Parkinson, *A Fluoride-Fuel In-Pile Loop Experiment*, ORNL-1965 (to be published).

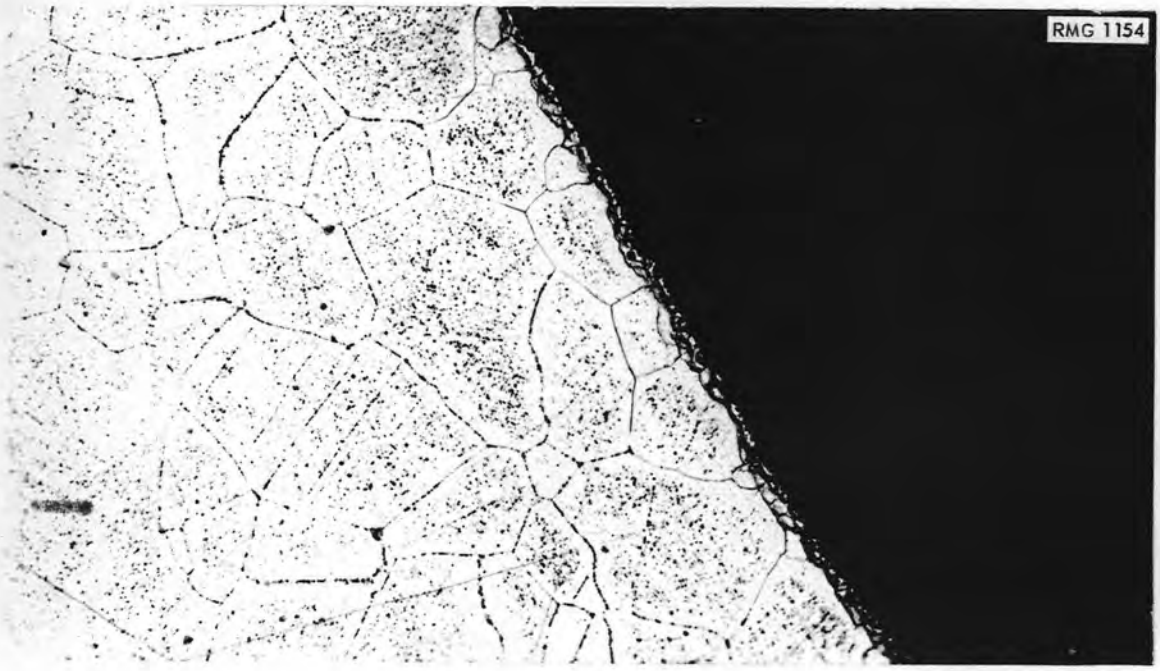

Fig. 8. Specimen 2, A Typical Sample from the Loop Between the Reactor Shield and the Pump. 250X.

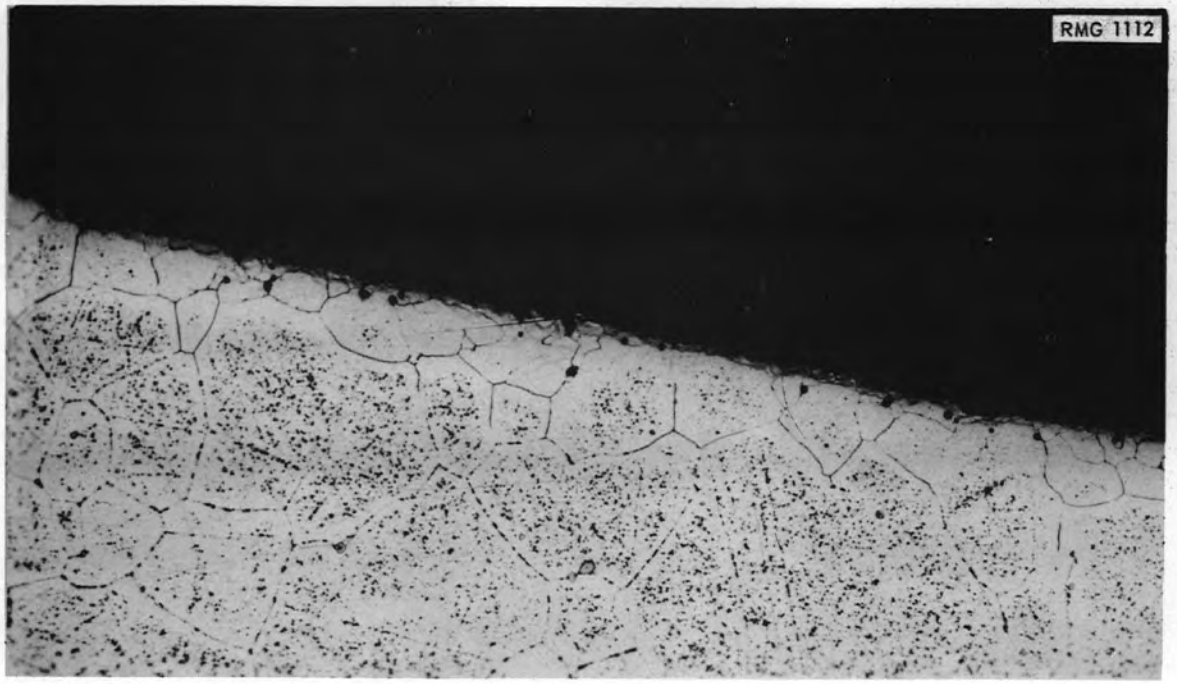

Fig. 9. Specimen 8, Taken from Loop Within the Reactor Shield. 250X.

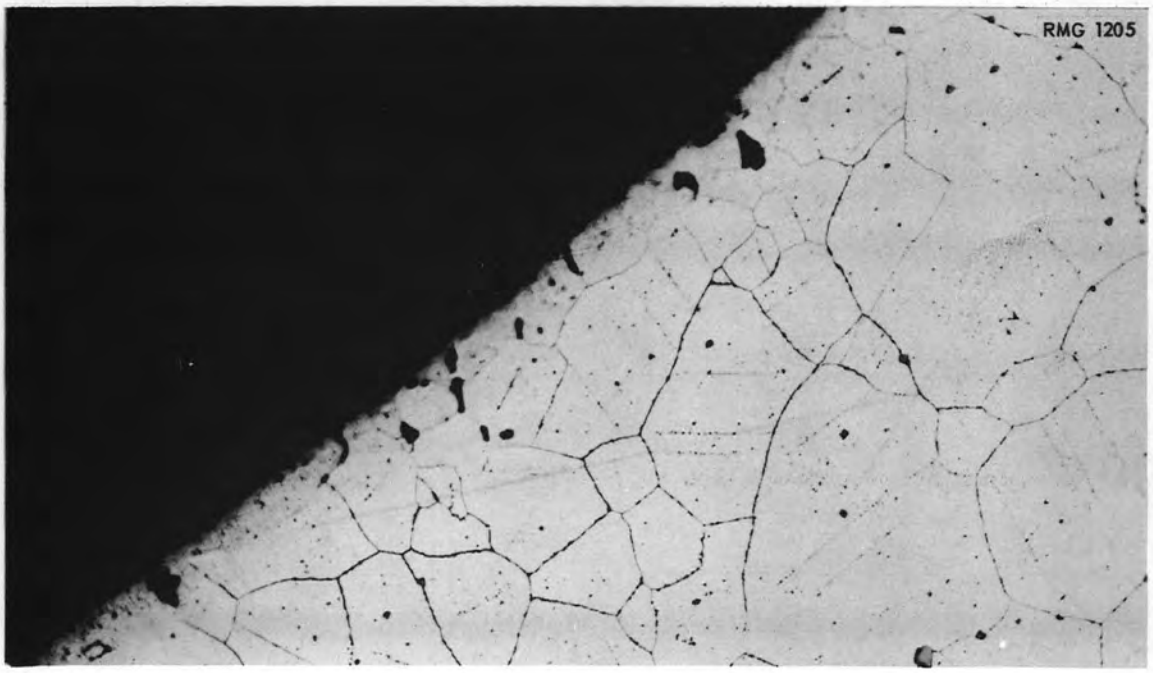

Fig. 10. Specimen 11, Taken from Outlet Line Within Reactor Shield, Shows Maximum Corrosion. 250X.

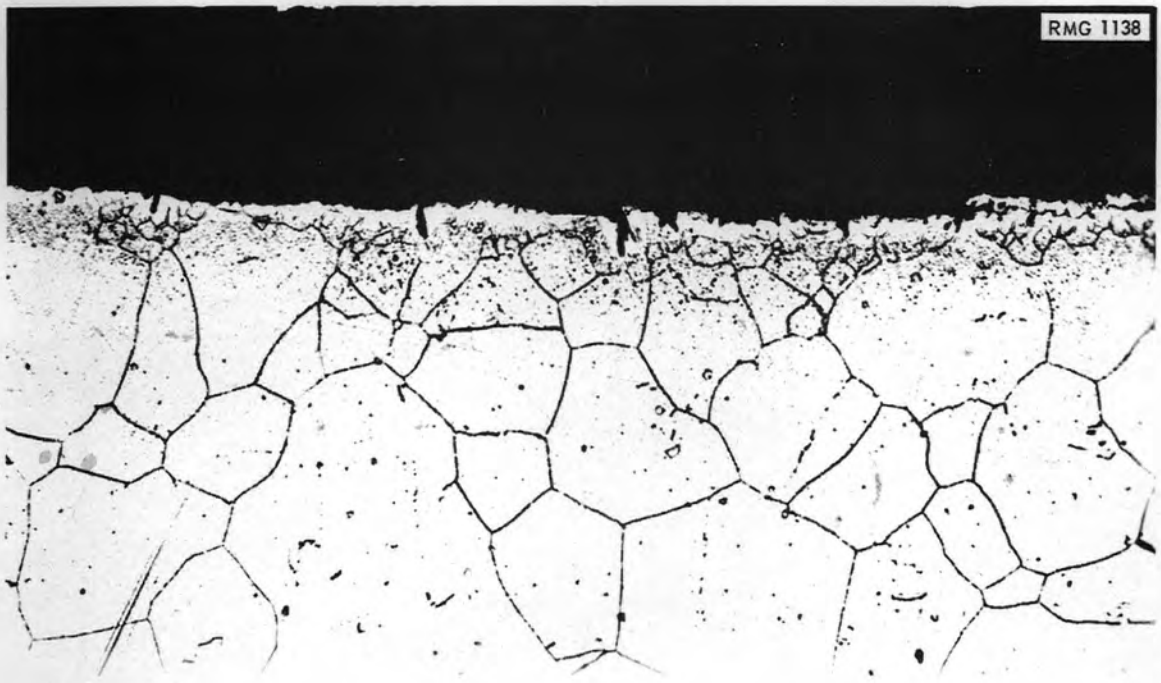

Fig. 11. Control Specimen 1B, Section of Outlet Line as Received. 250X.

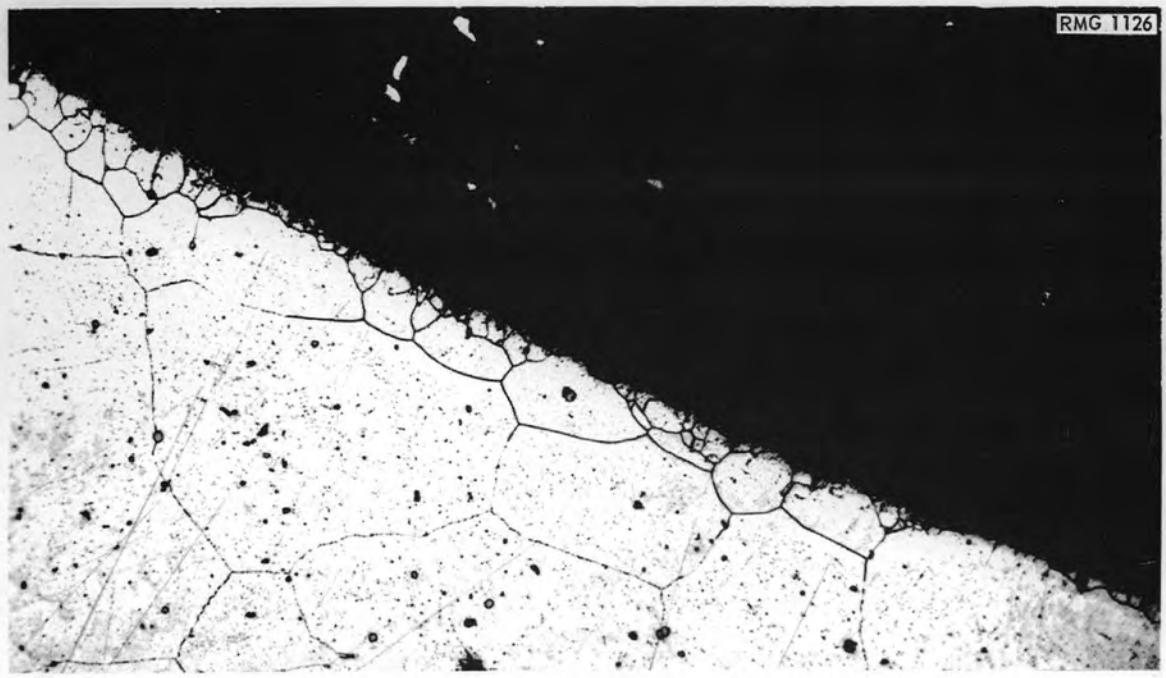

Fig. 12. Specimen 17, Exposed to the Greatest Flux in the Irradiated Section. 250X.

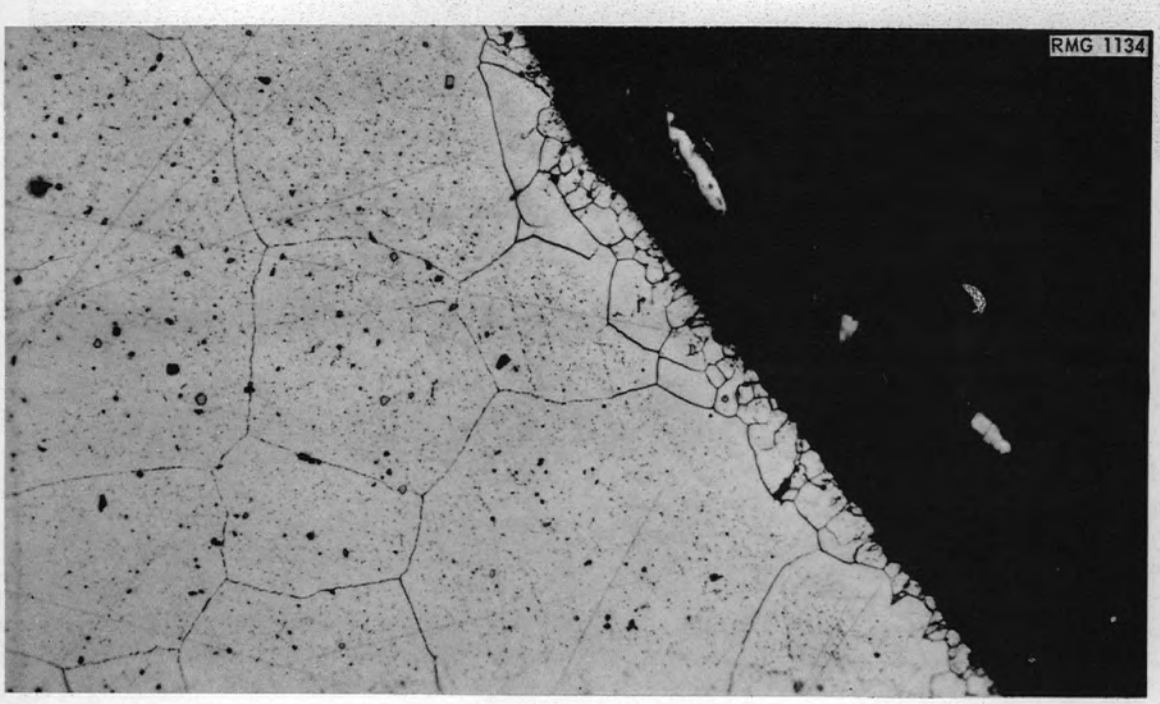

Fig. 13. Specimen 19, from the Outlet Leg of the Irradiated Section. 250X.

FUSED SALTS

G. W. Keilholtz

LITR VERTICAL DYNAMIC-CORROSION LOOP

W. R. Willis
M. F. Osborne
H. E. Robertson
D. E. Guss
C. C. Webster
A. S. Olson
C. D. Baumann

The vertical dynamic-corrosion loop described previously[1] has been operated in position C-48 of the LITR. Because of faulty behavior of the pump motor, the fuel flow velocity could not be maintained at a steady value, and the test was incomplete as a corrosion study. It was possible, however, to make a fairly thorough study of the in-pile characteristics of the loop. The test operated for a total of 30 hr at full power and with a fuel Reynolds number of 3200 to 5000. The operation throughout this period was complicated by intermittent motor trouble, and failure occurred when the motor stopped completely.

The instruments performed satisfactorily, controlling the temperature to ±5°F and not allowing excessive excursions in temperature when the fuel velocity changed rapidly. During the short run several scram situations occurred because of low pump speed, high activity in the off-gas stream, and because of a spurious high temperature that resulted from a thermocouple failure. All these situations were adequately handled in time to prevent high-temperature excursions.

The faulty behavior of the motor, the pressure transmitter on the venturi tube, and the header box in the off-gas system showed a need for some redesign. No complete explanation concerning the erratic behavior of the motor can be given yet, but it appears that the combination of a high temperature and a very dry helium atmosphere caused brush failure. The next test will use an induction motor with a canned rotor. It does not appear that any changes which could be made in the pressure transmitters in any reasonable time would be of much help, so the transmitters are to be removed from the system. Salt velocities will be estimated, as described later in this report. Removal of the pressure cells also allows more of the loop to be lowered into the reactor. This will increase the total power generation and will place the point of maximum temperature near the maximum neutron flux. The failure, during the short irradiation, of a gasket in the header box located at the face of the reactor allowed some leakage of activity into the mid-section of the LITR. The header box is to be redesigned to withstand full available air pressure without leaking.

Since the flowmeter was inoperable, another method of obtaining fuel velocities had to be devised. The method used was (1) to find the pressure developed at a given pump speed and (2) to find Δp vs flow for the loop. These values were measured by using water as the pumped fluid and exact duplicates of the pump and loop. Figure 14 shows a plot of pump speed vs Reynolds number of the salt. In Fig. 15 the temperature difference through which the salt flowed at a given Reynolds number and the values which were expected from the design calculations are compared.

The experimental ΔT shown in Fig. 15 is about 60% of the calculated value. This is considered to be a satisfactory check for two reasons: (1) the

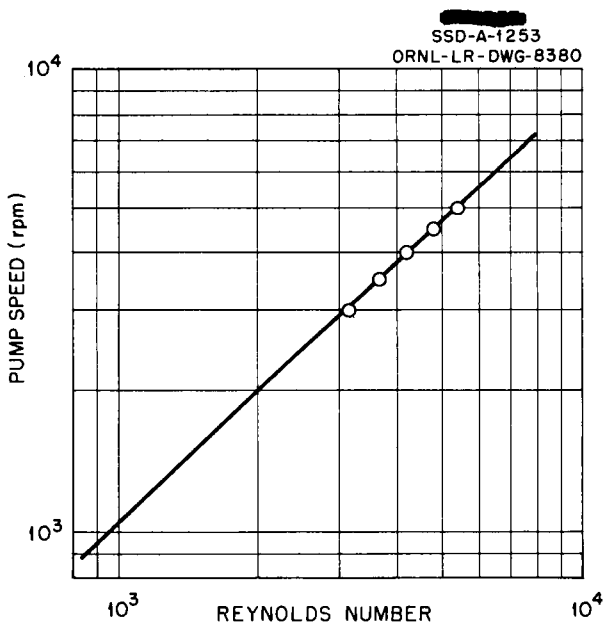

Fig. 14. Pump Speed vs Reynolds Number in the LITR Vertical Loop.

[1] W. R. Willis, *Solid State Semiann. Prog. Rep. Feb. 28, 1955*, ORNL-1851, p 13.

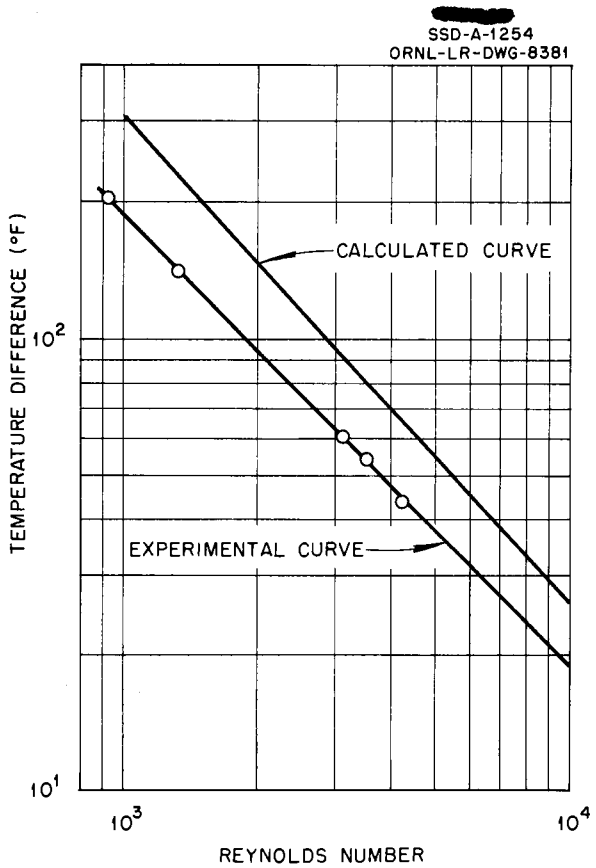

Fig. 15. Comparison of Calculated and Experimental Curves for Temperature Difference in the LITR Vertical Loop.

assumptions made in performing the design calculations[2] would tend to predict a value of ΔT higher than the experimental case, and (2) the uncertainty in many of the constants used decreases the accuracy of the calculation. Aside from these possibilities, the ΔT attained is directly proportional to the power generated in the loop. Thus, if the flux depression due to the loop was greater than estimated, or if the spatial distribution of the flux was greatly altered, a lowered ΔT would result. This possibility will be investigated when the values of the flux measured by a monitor in the loop are known.

The next loop will have a higher ΔT. This is because the loop will be inserted farther into the active lattice, and a higher flux will be available.

[2]M. T. Robinson and D. F. Weekes, *Design Calculations for a Miniature High-Temperature In-Pile Circulating Fuel Loop*, ORNL-1808 (Sept. 19, 1955).

DEPOSITION OF Ru^{103} AND Nb^{95} FROM FLUORIDE FUELS

M. T. Robinson T. H. Handley[3]
W. A. Brooksbank[3]

The deposition of the fission-product 40-day Ru^{103} on the surfaces of the fuel circuit of the ARE has been previously reported.[4] Confirmation of these results has now been obtained by study of samples from the horizontal fluoride loop operated recently in the LITR.[5] Two samples of pipe from this loop were examined by gamma-ray scintillation spectrometry: one (S_1) located upstream from the high-flux region of the loop, and the other (S_2) located an equal distance downstream.

No direct neutron activation of the elements of Inconel was observed. The results, corrected for differences in sample size, may be summarized as in Table 2. Within the experimental error, the Zr^{95}-Nb^{95} activity appears to be the same in the two samples. It is clear that Ru^{103} is deposited on the pipe, much as it was in the ARE. The sample downstream from the high-flux region contains markedly more Ru^{103} than does the upstream sample. This difference is exactly that expected for rapid reaction of ruthenium in the fuel with the container metals.

TABLE 2. ACTIVITY RATIOS FOR PIPE SAMPLES FROM INCONEL LOOP

Ratio of Activities	Samples		
	S_1	S_2	Calculated
Ru^{103}/Zr^{95}-Nb^{95}	5.33	8.07	0.6
$Ru^{103}/(Ru^{103})_{S_1}$	1.00	1.39	
Zr^{95}-$Nb^{95}/(Zr^{95}$-$Nb^{95})_{S_2}$	1.00	0.92	

Radiochemical analysis of a fuel sample for Ru^{103} indicated that the amount was below the limit of detection of the technique.[6] This demonstrates that the efficiency of ruthenium removal was comparable to that attained in the ARE.[4]

[3]Analytical Chemistry Division.

[4]M. T. Robinson, S. A. Reynolds, and H. W. Wright, *ANP Quar. Prog. Rep. March 10, 1955*, ORNL-1864, pp 13–15.

[5]O. Sisman *et al.*, *ANP Quar. Prog. Rep. March 10, 1955*, ORNL-1864, pp 150–155; *ANP Quar. Prog. Rep. June 10, 1955*, ORNL-1896, pp 163–167.

[6]W. W. Parkinson, personal communication.

The above data, together with operational and dimensional data from Parkinson,[6] have been used to estimate the rate constant for removal of ruthenium from the fuel in the loop. If the removal rate is assumed to be first order in Ru^{103} concentration, the half life for the process is about 0.5 min.

After a delay of 53 days, the two pipe samples were re-examined to determine the apparent half lives of the two components of the gamma-ray spectrum. For the Ru^{103} peak (0.50 Mev), the results, 42 days for sample S_1 and 43 days for sample S_2, amply confirm the assignment. For the Zr^{95}-Nb^{95} peak, however, the results were 40 and 43 days, respectively, instead of the near-65-day value expected. The contribution to this gamma-ray energy (0.78 Mev) must be largely due to 37-day Nb^{95}, the 65-day Zr^{95} being very low in relative amount (a few per cent). It appears very likely that niobium deposits along with ruthenium on the Inconel pipes. The deposition rate for Nb^{95} cannot be estimated, since it is produced very slowly from its Zr^{95} parent rather than rapidly from fission, as is the case with Ru^{103}.

Following this discovery, two of the ARE pipe samples were re-examined; the delay time was 130 days. The apparent half life of the 0.78-Mev gamma ray was 50 days in each case; whereas for the 0.50-Mev gamma ray the results were 51 days and 46 days. The first result seems to confirm the deposition of niobium on Inconel. The half life for the lower-energy peak is increased over the value observed above because of an increasing contribution of one-year Ru^{106}.

An autoradiograph of the third sample of ARE pipe is shown in Fig. 16. It is evident that under ARE conditions the Ru-Nb mixture does not diffuse readily into Inconel, the activity being well localized at the fuel-metal interface.

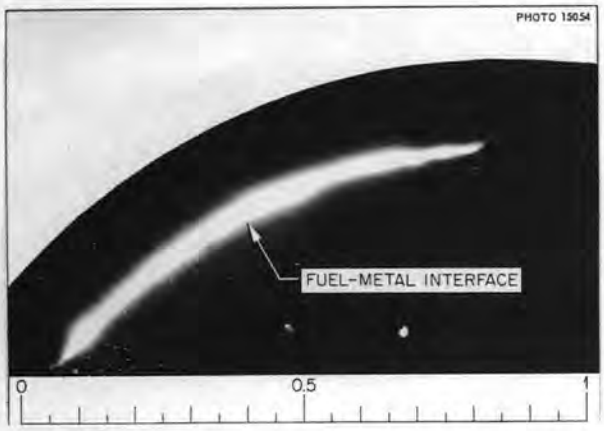

Fig. 16. Autoradiograph of an ARE Pipe Section.

THEORETICAL TREATMENT OF Xe^{135} POISONING IN THE ARE AND THE ART

M. T. Robinson

A theoretical study has been made of the kinetics of Xe^{135} poisoning in ANP-type reactors. The theory is presented in full in a separate report.[7] The system is assumed to consist of two phases, the liquid fuel and the sparging gas (helium). The theory is concerned only with volume-averaged concentrations and neutron fluxes. Turbulent motion of the two fluids is postulated in order to assure thorough mixing within each phase. On the basis of these assumptions the differential equations describing the behavior of the poisoning may be derived and solved. The various processes involved are illustrated schematically in Fig. 17.

The rates of all processes (except the two production rates) are assumed to be proportional to the Xe^{135} concentration in the initial phase. The rate constants for the two phase-transfer operations are related by application of the law of mass action, thus introducing the equilibrium solubility of xenon in the fuel.

Figure 18 illustrates the calculated dependence of the steady-state Xe^{135} poisoning on the sparging-gas flow rate for various assumed values of the phase-transfer mean life (the reciprocal of the rate constant for transfer of xenon from fuel to sparging gas). The time dependence of the Xe^{135} poisoning during reactor operation was studied by means of an extensive series of calculations performed on the Oracle.[8] Some typical results for the ART are shown in Fig. 19.

DELAY OF NOBLE GASES BY CHARCOAL TRAPS

D. E. Guss

In a flowing system, charcoal traps can be used to hold back noble gases for a period of time. The experiments described below were performed to provide data for the design of such a trap, which

[7] M. T. Robinson, *A Theoretical Study of Xe^{135} Poisoning Kinetics in Fluid-Fueled, Gas-Sparged Nuclear Reactors*, ORNL-1924 (in preparation).

[8] The coding and the computation of the problem was supervised by C. L. Gerberich, ORNL Mathematics Panel.

is to be incorporated into a fission-product off-gas line and operated at room temperature.

The experimental apparatus is shown schematically in Fig. 20. Ten-year Kr^{85} was introduced into a reservoir at the entrance to the trap and at zero time was driven through the trap with air. It then passed through a flowmeter and then through a counter, where the activity of the eluted gas was determined as a function of time.

Runs were made at various air flow rates on two small, cylindrical charcoal traps: one, 2.25 in. long by 1.05 in. in diameter; and the other, 23.5 in.

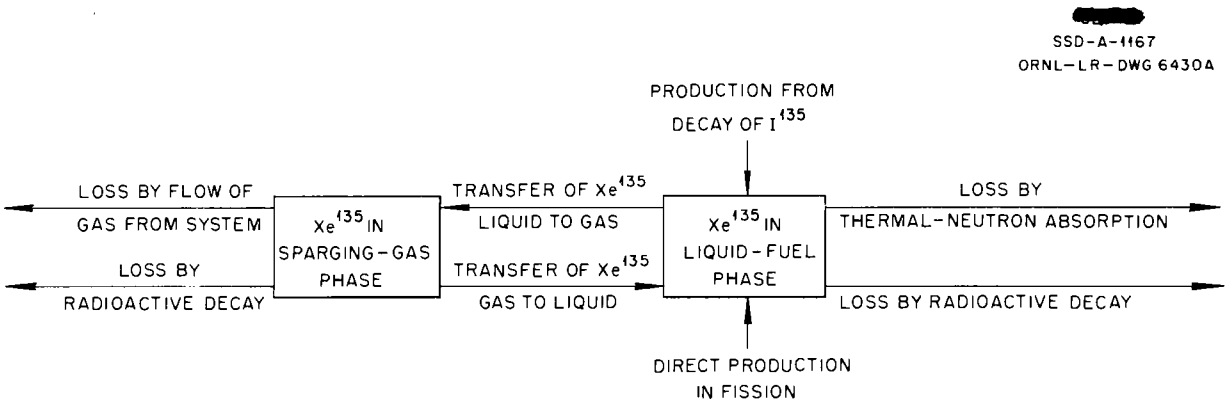

Fig. 17. Processes Governing Xe^{135} Poisoning in Fluid-Fuel Reactors.

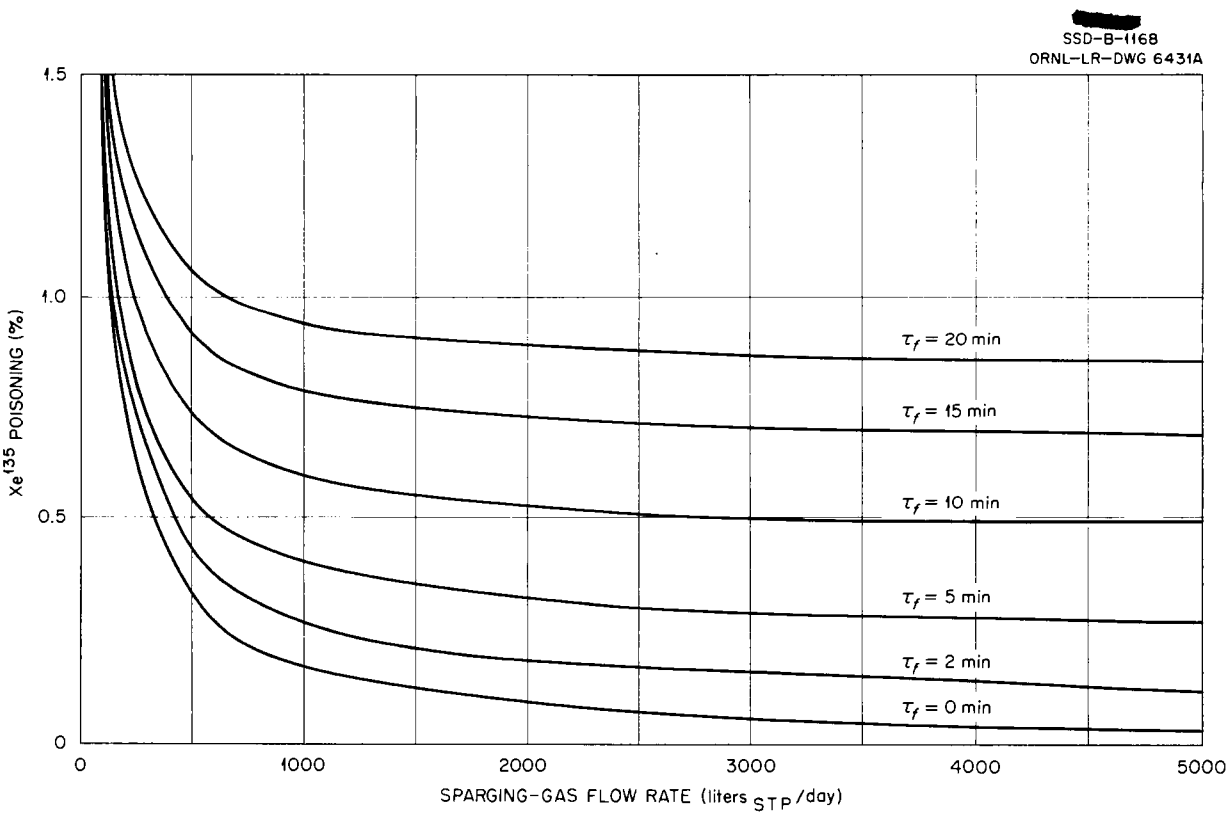

Fig. 18. Steady-State Xe^{135} Poisoning in the ART as a Function of Sparging-Gas Flow Rate for Various Assumed Values of the Phase-Transfer Mean Life, τ_f.

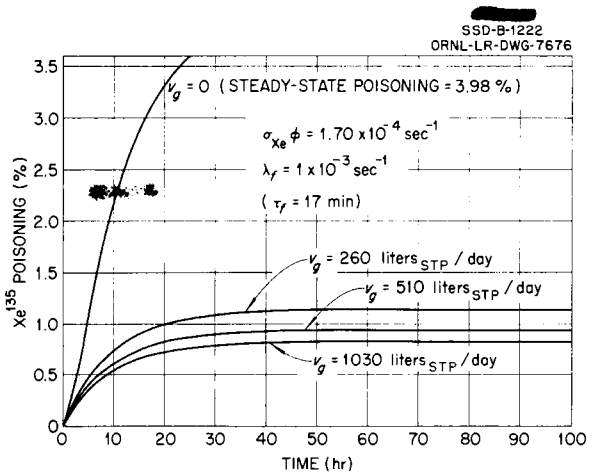

Fig. 19. Effect of Sparging-Gas Flow Rate on ART Poisoning.

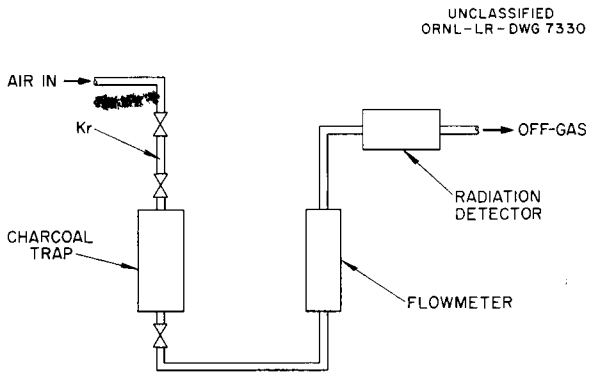

Fig. 20. Schematic Diagram of Charcoal-Trap Experiment.

long by 1.05 in. in diameter. In addition, a trap 24 in. long by 10 in. in diameter was used at a single air flow rate (19.9 cfm). The traps contained 0.48 g/cc of 6 to 14 mesh activated coconut charcoal with an N_2 surface area of 1150 m^2/g. All the runs were made at room temperature.

According to a treatment by Mayer and Tompkins[9] and based on an analogy of the column separator to a fractionating distillation column, the maximum of the elution peak occurs at that number of column volumes which in any theoretical plate is equal to the ratio of the solute in the solid absorbent to the solute in the fluid phase. Since the ratio of the partial pressure of the noble gas in the gas phase to the partial pressure of that absorbed is a constant at a given temperature over an extremely wide range of noble-gas partial pressures, the relationship between air flow rate and the time, t, for the elution to peak for a particular trap can be expressed as $t = KV/f$, where f is the sweeping-gas flow rate, V is the trap volume, and K is a proportionality constant which is dependent upon the particular charcoal used, the trap temperature, the noble gas under consideration, and the way the charcoal is packed into the trap.

The trap should be somewhat (perhaps by a factor of four) longer in the direction of flow than it is in diameter, because entrance effects for a short trap lessen the effectiveness of a portion of the charcoal and cause the elution peak to occur before the time predicted by the above equation. This was observed in the 2.25-in.-long by 1.05-in.-dia trap though not in the 23.5-in.-long by 1.05-in.-dia trap.

For a particular trap, the equation shows that a plot of time to reach the elution peak vs flow rate should be linear. These plots for the 23.5 × 1.05 in. trap and the 2.25 × 1.05 in. trap are shown in Figs. 21 and 22, respectively. An extrapolation of the line in Fig. 22 does not intercept the origin for the reason noted above.

In the one run made on the 24-in.-long by 10-in.-dia trap, the experimental elution peak occurred at the time (within experimental error) predicted by the equation in which the value of K was used that had been determined by the experiments run on the smaller traps.

A typical elution curve is shown in Fig. 23, in which the time coordinate is expressed in trap volumes of eluted gas rather than in seconds. The elution curves retain the same general shape at any flow rate but become more symmetrical as the flow rate decreases. The amount of rare gas eluted before the peak ranged from about 0.35 of the total to about 0.45 of the total as the flow rate was decreased from 0.3 trap volume/sec to 0.03 trap volume/sec. The leading edge of the elution curve was approximately linear, but it was distorted into a slight S-shape at the highest flow rates that were run (0.3 trap volume/sec), the initial breakthrough coming sooner. This perhaps occurs because complete equilibration between the gas phase and the absorbed phase does not occur at high flow rates. A similar distortion could be expected at

[9] S. W. Mayer and E. R. Tompkins, *J. Am. Chem. Soc.* **69**, 2866 (1947).

very [redacted] flow rates, where diffusion becomes important, but this was not observed at the lowest flow rate that was run (0.03 trap volume/sec).

Although these experiments were run by using a pulse of active krypton, a charcoal trap can be used to delay rare gases flowing continuously through the trap, and it acts on each segment of the stream as it does on a pulse.

Two [redacted] in.-long by 10-in.-dia charcoal traps were installed in series on the off-gas system of the vertical in-pile loop at the LITR. During operation of the loop several bursts of fission-gas activity occurred. The time lag between the appearance of the activity at a monitor just upstream of the traps and the monitor at the off-gas stack was consistent with the experiments described.

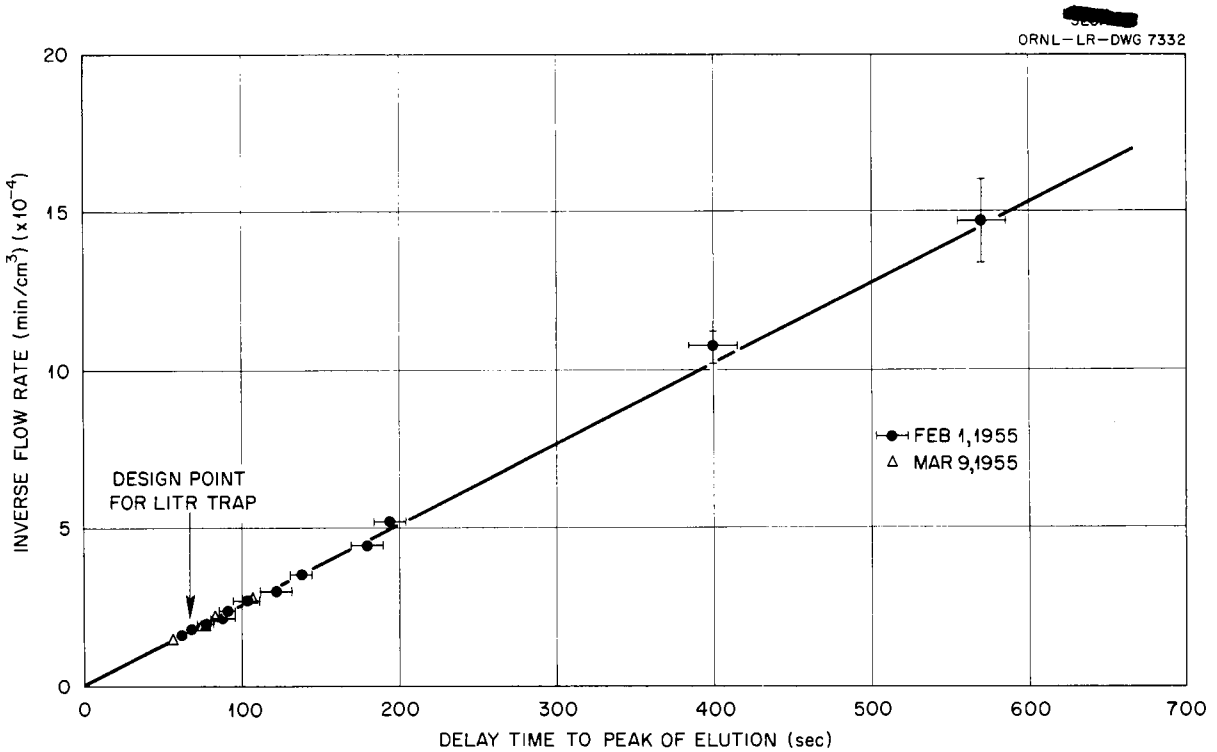

Fig. 21. Inverse Air Flow Rate vs Time to Peak Activity for a 23.5-in.-long, 1.05-in.-dia Charcoal Trap Containing Krypton.

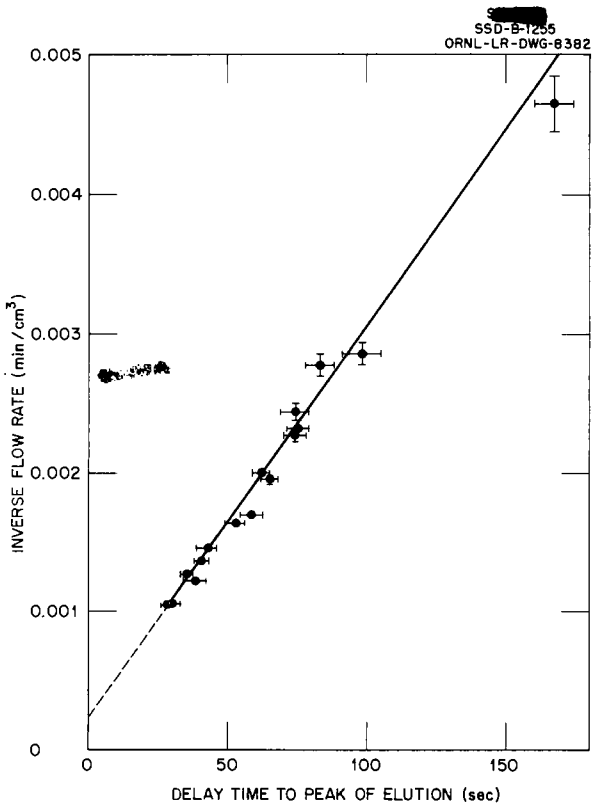

Fig. 22. Inverse Air Flow Rate vs Time to Peak Activity for a 2.25-in.-long, 1.05-in.-dia Charcoal Trap Containing Krypton.

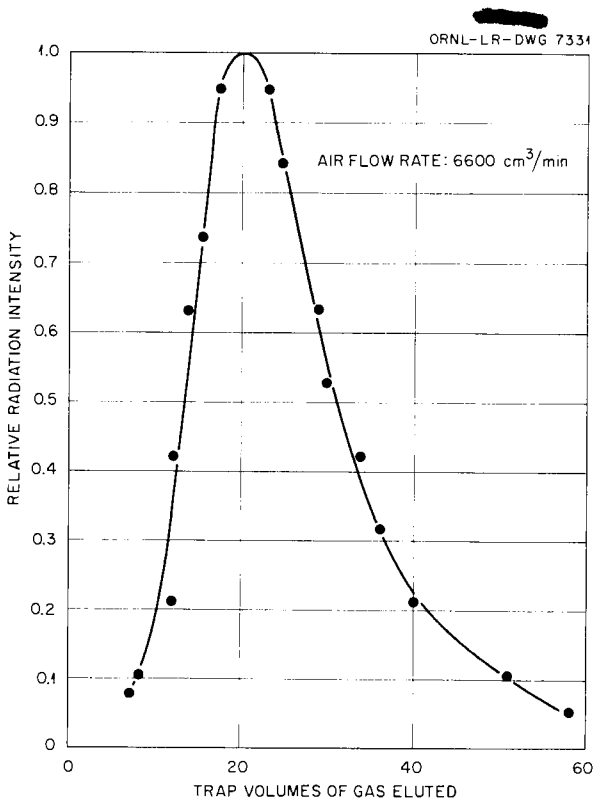

Fig. 23. Elution Curve for 334-cm³ Charcoal Trap Containing Krypton.

SPECIAL PROJECTS

HOT-CELL OPERATION

S. E. Dismuke M. J. Feldman
E. S. Schwartz

HRP in-pile loops FF, GG, and EE[1,2] were disassembled in the hot cells under the direction of A. R. Olson, Reactor Experimental Engineering Division. This operation not only involved the removal of samples from the core and in-line sample holders but also involved weighing, defilming, inspecting, photographing of the samples, and sectioning of the sample holders. In addition, other portions of the loops were sectioned and inspected in the hot cells after preliminary dismantling had been performed in the remote cell in Building 4501. These portions included the pressurizer, pressurizer heater, pump, and a section of the line including the sample-line filter.

In an experiment conducted by C. D. Watson of the Chemical Technology Division, the side plates from an irradiated LITR fuel element had to be removed. This was accomplished on the remotely controlled milling machine by the use of a specially designed jig and twin milling cutters. The sides of the element were successfully milled off to a depth of nine fuel plates without cutting into uranium in any of the plates. The combs on the ends of the fuel plates were cut off with a small hand shears modified to operate with the General Mills manipulator. Another phase of the same experiment, results of which have not as yet been correlated, involved shearing, bending, and pressing sample sections of these fuel plates, both in air and under water. This work was also performed in the hot cell.

The LITR fluoride-fuel loop discussed previously[3] was disassembled in the hot cells under the direction of R. M. Carroll and W. W. Parkinson. This extensive operation was completed with little difficulty, although four days were lost due to manipulator breakdowns. It is believed that the design changes in the new General Mills manipulator, which will be delivered about September 1, will eliminate the causes of these breakdowns. An electric arc was successfully used to cut the stainless steel pump jacket. To start the arc, it was necessary to use a high-frequency signal, since the manipulator could not be controlled with enough sensitivity to draw an arc. Other difficulties in this operation were primarily concerned with manipulation techniques and were overcome through practice.

The final two capsules (PW-1-12 and PW-1-13) of the Supercritical Water Reactor experiment were received. The samples were removed without difficulty and were prepared for metallographic analysis; the results will be discussed in a later report. The chemical analyses and uranium-burnup determinations on samples from these capsules, neither of which have been completed, will conclude ORNL's participation in this experiment. Uranium-burnup determinations on samples from capsules PW-1-10 and PW-1-11 were reported,[4] thus completing the data on these capsules.[5,6]

Impact and tensile measurements were conducted on various irradiated metals for both the ANP and HRP by J. C. Wilson. In addition, tests were also conducted for J. J. Lombardo, Westinghouse Atomic Power Division, Pittsburgh, Pa. The specimens for this experiment were removed from their irradiation facilities in the remote machine shop by using the lathe and milling machine to open the containers.

The equipment described previously[7] for dismantling the miniature dynamic-corrosion loops was installed in cell 6 under the supervision of C. C. Webster. This equipment includes the band saw, tube furnace, and a shielded storage facility.

Due to the high dose rate and excessive fission-gas activity expected from these loops, other changes were necessary in the cell proper. An additional shield of 2 in. of lead was installed

[1] H. C. Savage, G. H. Jenks, *et al.*, *HRP Quar. Prog. Rep. Jan. 31, 1955*, ORNL-1853, pp 86–106.

[2] H. C. Savage, G. H. Jenks, *et al.*, *HRP Quar. Prog. Rep. April 30, 1955*, ORNL-1895, pp 94–117.

[3] W. E. Brundage *et al.*, *Solid State Semiann. Prog. Rep. Feb. 28, 1955*, ORNL-1851, pp 7–12.

[4] E. S. Schwartz, *Results of Uranium Burnup Determinations for Capsules PW 1-5, PW 1-8, PW 1-10, and PW 1-11*, ORNL CF-55-5-18 (May 3, 1955).

[5] M. J. Feldman *et al.*, *Metallographic Examination of P&W Capsules 1-10 and 1-11*, ORNL CF-54-12-212 (Dec. 29, 1954).

[6] R. M. Hawkins, E. S. Schwartz, and R. E. Mayes, *Post-Irradiation Studies of Pratt and Whitney Aircraft Solid Fuel Element Capsules PW 1-5, PW 1-8, PW 1-10, and PW 1-11*, ORNL CF-54-12-81 (Dec. 10, 1954).

[7] C. C. Webster and A. F. Zulliger, *Solid State Semiann. Prog. Rep. Feb. 28, 1955*, ORNL-1851, pp 24–27.

on the roof of the cell. Also, a plywood canopy 2 in. thick was installed over the operating area in front of the cell. it is believed that these will serve to reduce the effect of scattered radiation passing through the roof manipulator ports. The use of closed-circuit television to monitor the dismantling operation is also under investigation as an alternative in the event that the scattered radiation too severely limits the operating time.

Plastic boots were installed on the manipulators to close the manipulator ports in the roof, and this improved the cell off-gas characteristics considerably. It is planned to make this modification in the other master-slave cells also.

Experience during the first six months of this year has indicated that actual experimental operations account for only about 25% of the hot-cell time available for an experiment. Actual experimental operations in this case include only those tests and operations performed on active samples. Not included are such operations as installation and testing of experimental equipment, in-cell bench tests, emergency and scheduled maintenance, removal of material and equipment, and decontamination of the cell. These operations require the remaining 75% of the available cell time.

The above information was obtained by maintaining an accurate day-by-day log on each of the seven hot cells in use during the first six months of the year. A careful record was kept, showing how each cell was used and the responsible personnel in charge.

HOT METALLOGRAPHY

M. J. Feldman R. N. Ramsey
A. E. Richt W. B. Parsley
E. J. Manthos

Work has continued on the examination of specimens from the HRP groups. Examination of components from in-pile loop FF has been completed and reported.[8] Examination of the corrosion coupons from this loop has been delayed until completion of the metallographic-cell extension.

Examination of sections from the LITR fluoride-fuel loop No. 2 has been completed and reported.[9] Examination of sections of the tubing used in construction of the loop revealed that surface cracks were present on the inner wall of the tubing prior to operation of the loop. Depth of corrosive attack was slight, and only small variations were found along the length of the loop. The area showing maximum depth of corrosive penetration was on the outlet line some 3½ ft from the nose of the loop.

Examination of two fuel elements for the GE-ANP Division has been completed, and the data have been reported.[10] These elements failed during exposure in the MTR, and examination was desired in order to determine the cause of failure. The core of both elements was found to contain significant amounts of unalloyed chromium and stringers of what is thought to be chromic oxide. As a result, these failures could not be attributed to radiation damage even though a significant increase in hardness of the cores was noted. Similar unirradiated elements tested by G.E. also failed in a like manner.

Sections of an MTR fuel element which had failed in operation were also examined, and the results have been reported.[11] Metallographic examination substantiated the MTR theory[12] in which failure was attributed to environmental causes rather than to radiation damage. Figure 24 shows a montage of the sections examined. Figure 25 is a reconstruction of one of the examined sections in which the sample has been projected into its as-irradiated condition.

Examination of sections of LITR element L-33 has been completed, and the results have been reported.[13] The purpose of this experiment was to determine the feasibility of bending the element plates for ease in chemical processing. Sections of plates were annealed and bent; then they were examined in order to ascertain the effects on plate integrity. General conclusions were that, although

[8] M. J. Feldman *et al.*, *Metallographic Examination of HRP In-Pile Loop "FF" Components*, ORNL CF-55-5-154 (May 16, 1955).

[9] M. J. Feldman *et al.*, *Metallographic Analysis of Fuel Loop II*, ORNL CF-55-6-22 (June 21, 1955).

[10] M. J. Feldman *et al.*, *Metallographic Examination of GE-ANP-3U and GE-ANP-30 Fuel Elements*, ORNL CF-55-3-107 (March 15, 1955).

[11] M. J. Feldman *et al.*, *Metallographic Analysis of Sections 1, 2, 3 of MTR Element 1-700*, ORNL CF-55-3-182 (April 29, 1955).

[12] J. B. Burham, M. H. Bartz, and O. J. Elgert, "Break in Cladding of MTR Fuel Element," presented at AEC Metallurgy Conference, Oak Ridge, April 1955 (to be published by TIS).

[13] M. J. Feldman and E. J. Manthos, *Metallographic Analysis of LITR Element L-33*, ORNL CF-55-5-116 (May 17, 1955).

[redacted]

[redacted]
RMG 1084

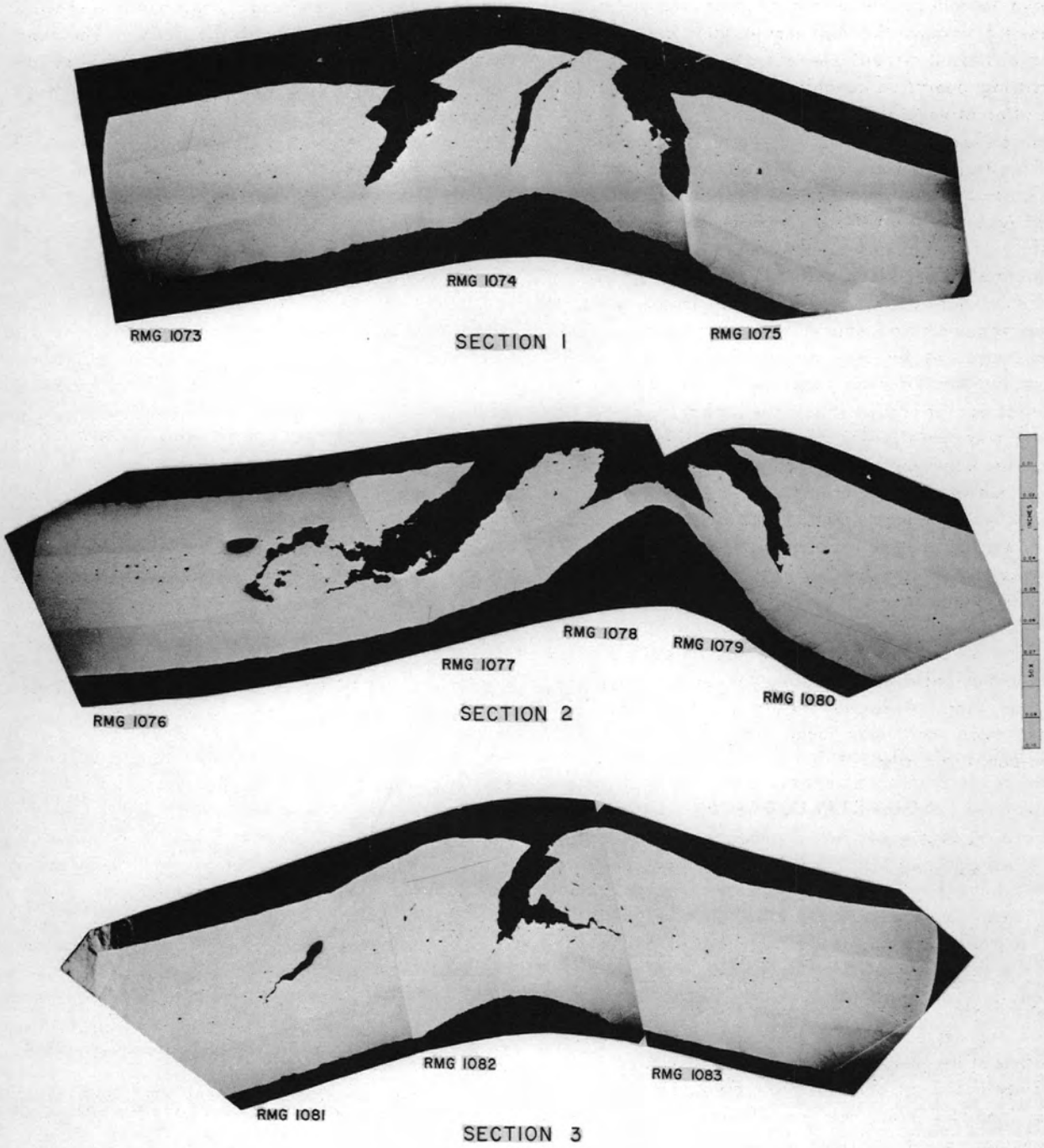

Fig. 24. Montage of MTR Fuel-Element Sections.

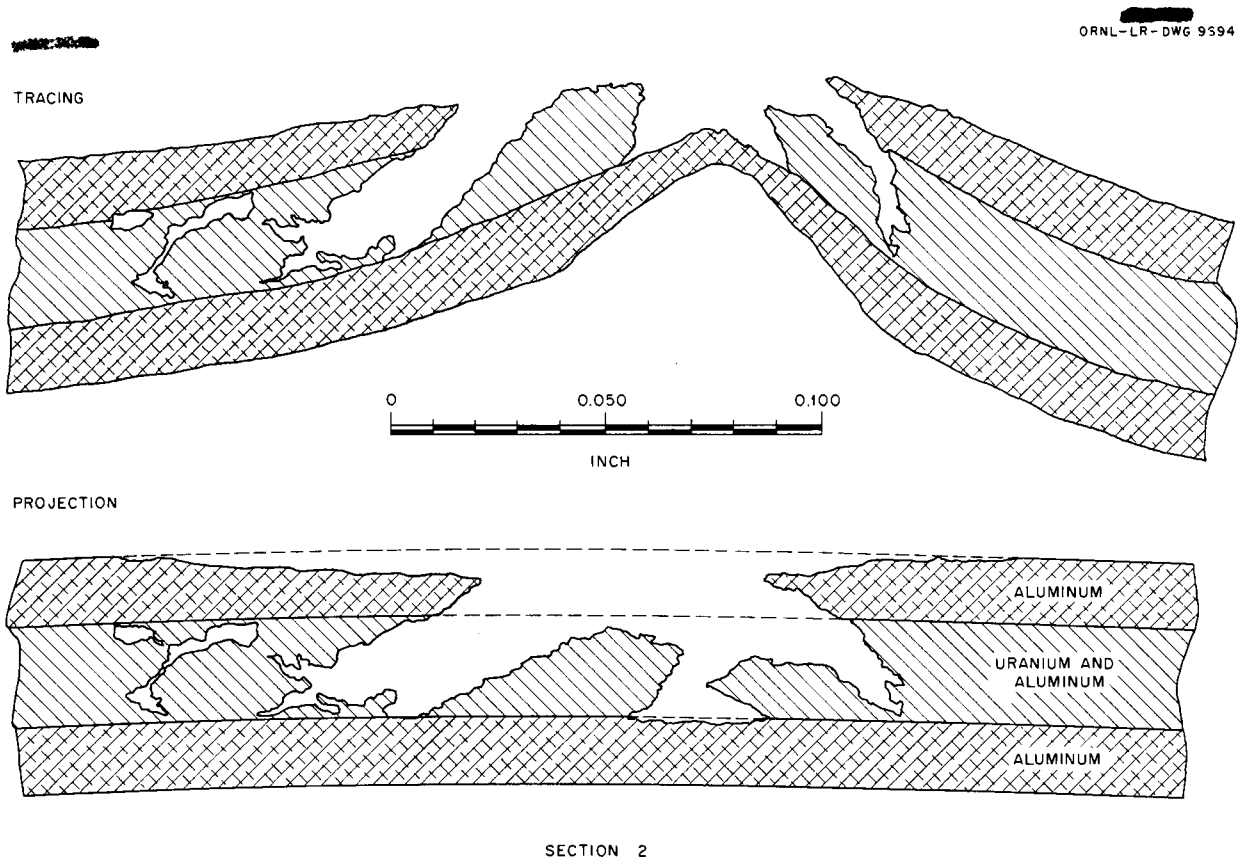

Fig. 25. Reconstruction of Section 2 of Fig. 24.

annealing did improve the ductility of the plates, the bends that were necessary for the application under investigation were beyond the limits of the ductility of the irradiated and annealed samples.

In conjunction with the ARE Division, the Remote Metallography Group has assumed the responsibilities for the postirradiation handling of the MTR-irradiated in-pile loops. Initial sectioning of the loops will be done at the G-E facility at the Reactor Testing Station, Idaho Falls, under the direction of C. Durrill, with technical assistance from the Remote Metallography Group. Final sectioning and metallographic analysis are to be done in the Solid State Division hot cells.

As had been reported in the previous three semiannual reports,[14–16] design and development work had been undertaken for the extension of the existing remote metallographic facilities and for the installation of new equipment. Remote operations were stopped on May 2, the cell was thoroughly decontaminated, and actual construction was started on May 16. Shielding construction was completed by June 1, and the cell auxiliaries were installed by July 1. Equipment and service installation was completed by August 1. Complete installation and alignment of equipment will be realized by August 15, and, with one week allowed for cold operation, the first hot work is estimated to begin on August 23.

The redesign and extension of the remote metallographic facility were prompted by an increase in demand for metallographic analyses of irradiated experiments. The demand not only created an increased amount of work but also required the

[14] M. J. Feldman, *Solid State Semiann. Prog. Rep. Feb. 28, 1954*, ORNL-1677, p 12.

[15] M. J. Feldman and R. Hawkins, *Solid State Semiann. Prog. Rep. Aug. 30, 1954*, ORNL-1762, p 17.

[16] M. J. Feldman *et al.*, *Solid State Semiann. Prog. Rep. Feb. 28, 1955*, ORNL-1851, p 6.

handling of a wider range of materials. The most feasible method of expansion was to extend the present facility. For expansion design purposes, the metallographic process was considered as being divided into three operational stages; and the needs and modifications of each were considered.

The first stage, the mechanical operations, is most suited to automation. This portion of the process, because of the large amount of radioactive material it must handle, requires substantial shielding. For these reasons the equipment for cutting, mounting, lapping, and polishing remained in the original metallographic cell, where the existing 3-ft concrete walls afford adequate shielding.

The chemical and optical operations, the second and third stages of the process, had been successfully operated in the old facility but had suffered from their proximity to the mechanical operations. For this reason and also because of the very limited operating area of the original setup, an extension to the cell was designed to contain the chemical and optical stages.

The chemical section of the extension is lined with stainless steel and is serviced with a model 4 master-slave manipulator. It has a separate ventilating duct to ensure the removal of the harmful vapors from the etching operations. Also included in the design was an elevating section of the floor for the quick insertion of chemical solutions. The chemical section and the main cells are connected by means of an endless-belt conveyor. In addition, in order to determine the quality of the sample before it is transferred to the optical cell for photography, a Bausch and Lomb model GBILS metallograph has been adapted for direct viewing of the etched samples in the cell by means of a through-the-wall extension to the photographic ocular.

The basic design of the cell extension was predicated on the needs of the optical section of the cell extension: more specifically, that a research metallograph would be incorporated into the cell in such a way as to include the stage of the metallograph in the cell proper and at the same time have the light source, bellows and ground glass, and direct-viewing ocular on the outside of the cell. Figures 26 and 27 show the metallograph as it was installed. For maintenance and repair, the

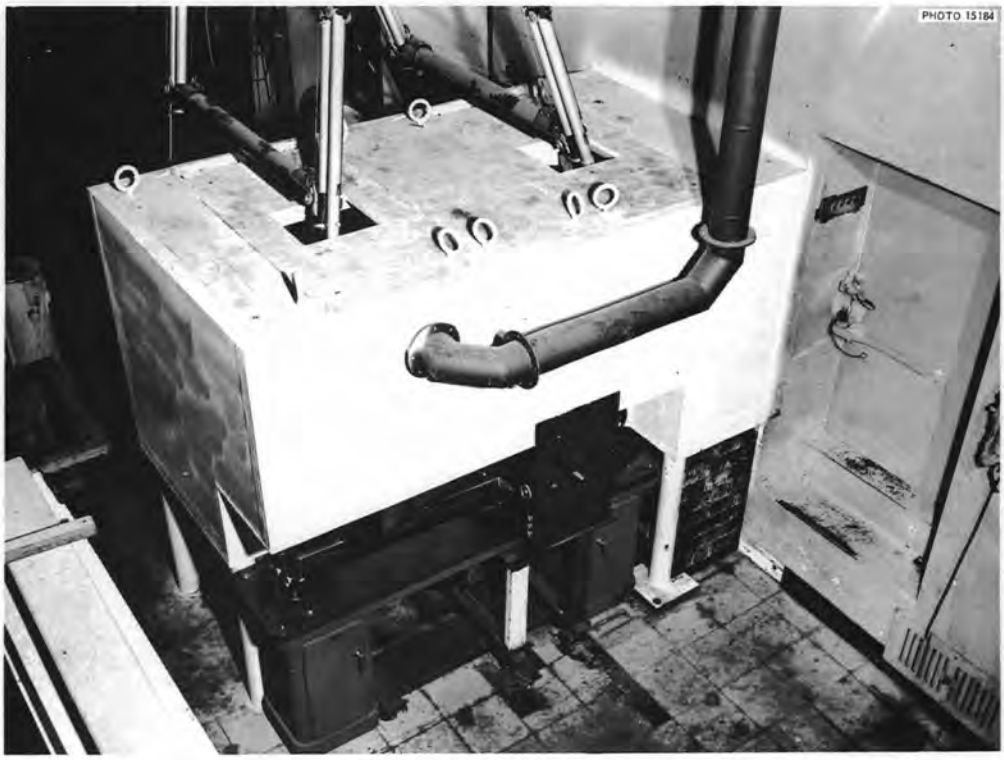

Fig. 26. Metallograph Viewed from the Rear of the Hot Cell.

metallograph and its shield can be removed from the cell proper. Also included in the optical section are the stereoscopic viewing unit and the Tukon hardness tester. The endless-belt conveyor, which is used to transfer the samples to the chemical cell, passes through the optical cell. Moreover, in this way transfer between any of the three cell sections can be easily accomplished.

In conjunction with the design and installation of an extension to the metallographic cell, a redesign of a major portion of the existing equipment was undertaken. In planning this redesign, advantage was taken of the experience gained in working with this equipment for the past three years. Since the major source of personnel irradiation has occurred during maintenance in the course of operation, an attempt was made to incorporate, in the design changes, provisions for easier maintenance. Each individual piece of equipment was unitized; that is, mounting and service connections are separate from any of the other pieces in the cell.

In addition to unit design, what is referred to as modular construction was used. For the modular construction of remote equipment, the operation of the machine is analyzed, and then the machine is designed so that each part that performs a major motion (and therefore a point of potential difficulty) is built as a separate module which can be quickly removed from the unit for maintenance. Where it is feasible, spare units of the major items of the modular equipment are kept on hand. In this way, maintenance periods of long duration within the cell are minimized. A defective module of a piece of remote equipment can be quickly replaced; operations can resume; and necessary repairs can be made outside the cell at a convenient time and after decontamination of the part. Figure 28 shows the in-cell portion of the ultrasonic specimen cleaner. Figure 29 shows schematically the modular construction of this piece of equipment. An attempt is being made to build all new equipment by modular construction, and some redesign was undertaken to approach modular construction on the older equipment.

The cost of incorporating these remote-equipment features into the facility is low. On a newly designed unit the increase in cost is negligible, and another advantage is that the machines are kept

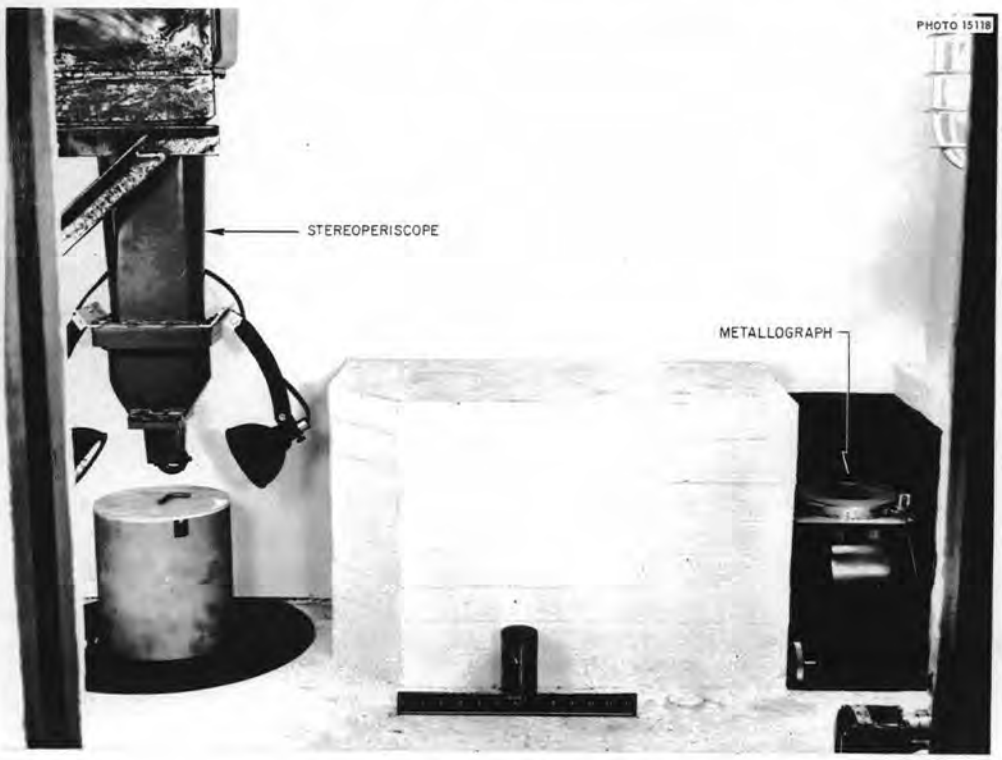

Fig. 27. Metallograph Viewed from Within the Hot Cell.

simple. On a redesigned unit the added cost is estimated to be less than 5% greater than the original cost, and the dimensions of the machine are estimated to have increased less than 10%. This cost is felt to be small when judged from the standpoint of reduced personnel irradiation and the reduced time loss in the course of performing maintenance that is required within the cell.

PHOTO 13730

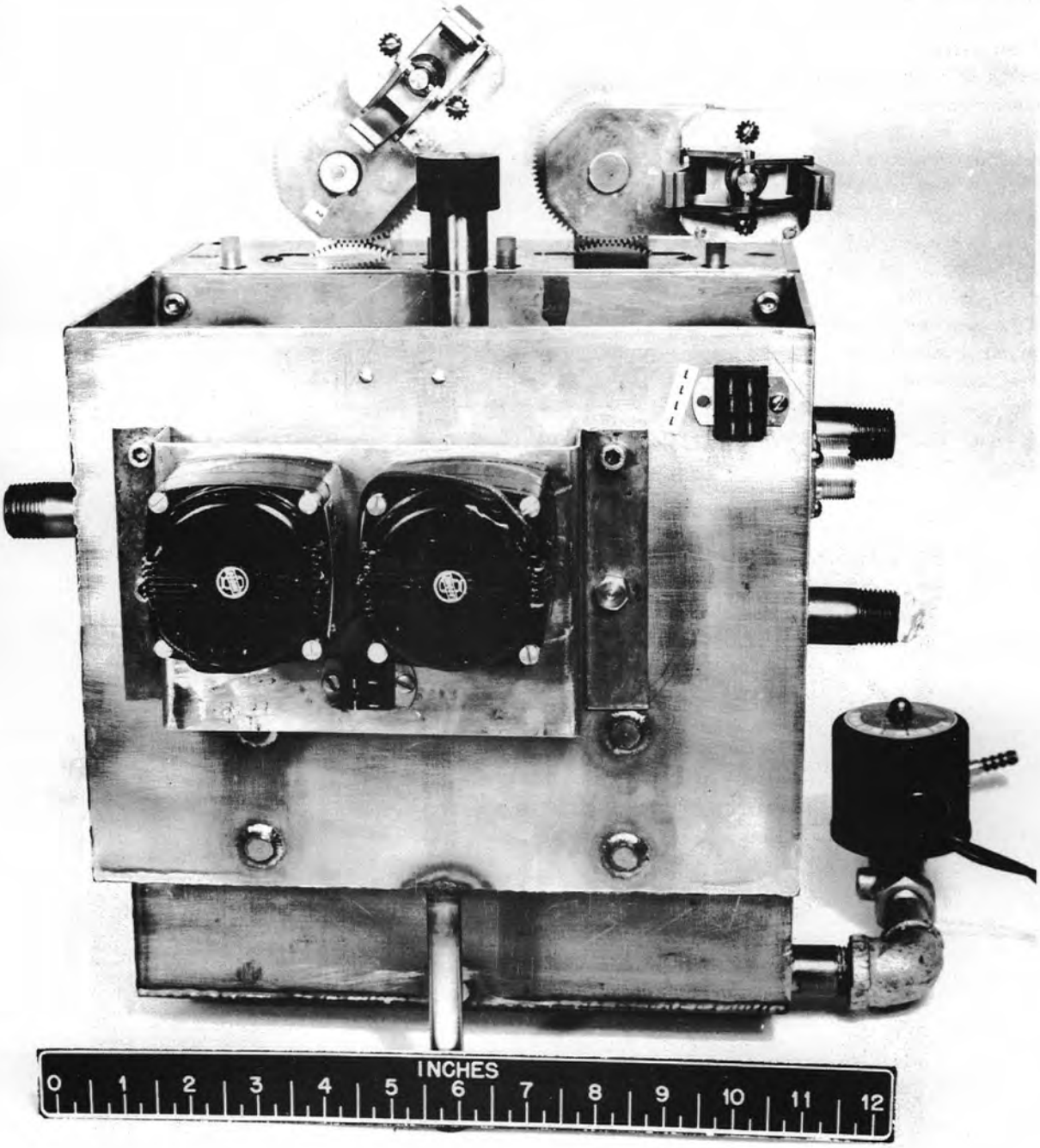

Fig. 28. In-Cell Portion of the Ultrasonic Cleaner.

[redacted]

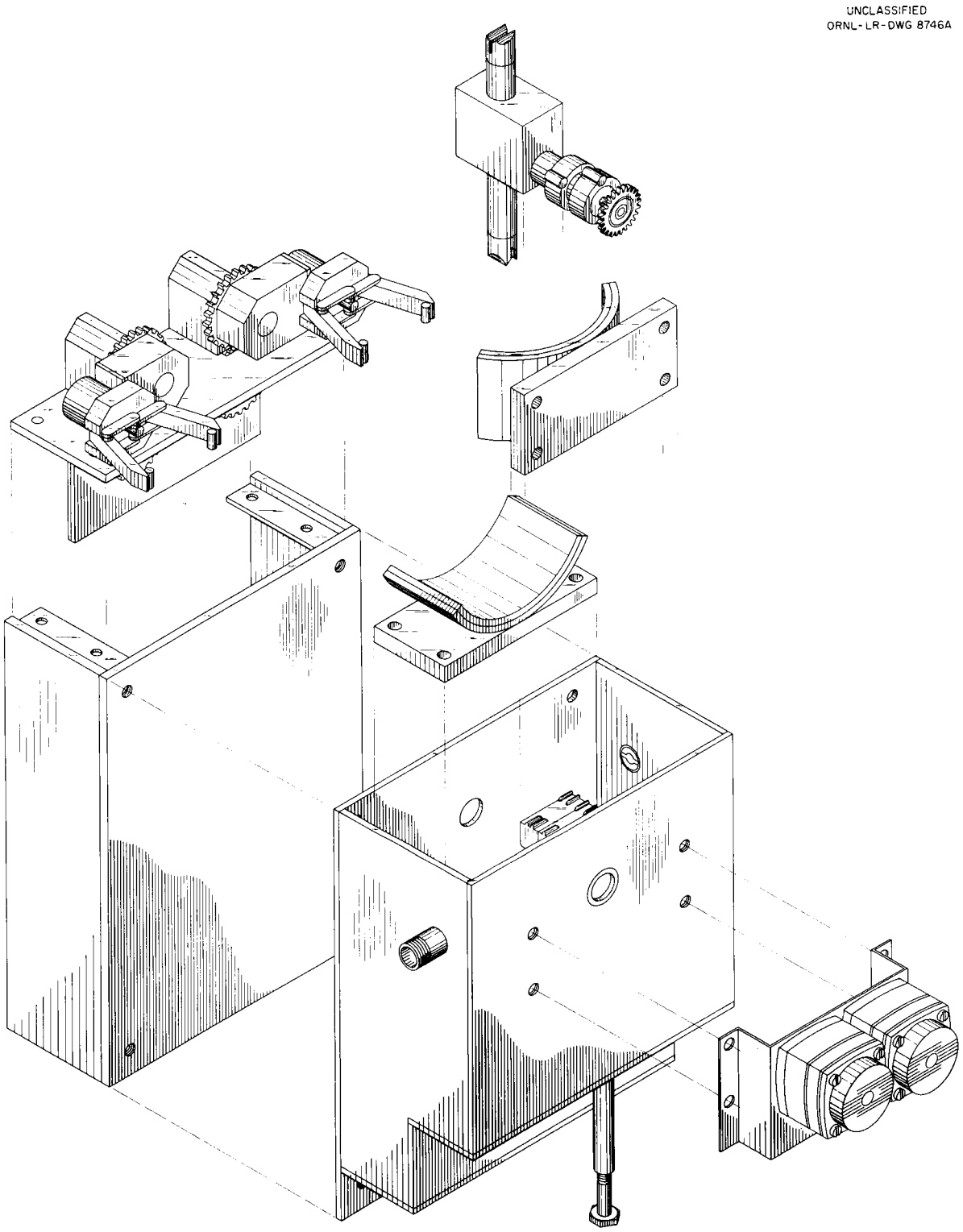

Fig. 29. Schematic Representation of the Ultrasonic Cleaner Showing the Modular Construction.

[redacted]